Chemico-structural degradation of Carboniferous lingulid shells

MAGGIE CUSACK AND ALWYN WILLIAMS

Department of Geology and Applied Geology, University of Glasgow, Glasgow G12 8QQ, U.K.

SUMMARY

Shells of *Lingula squamiformis* from argillaceous sediments at three horizons within the Dinantian Series, exposed at three localities in Scotland, have been studied to determine chemico-structural changes resulting from fossilization. Biomineral structures are essentially the same as those of living *Lingula anatina* with apatitic granules aggregating into spherules, up to 60 nm in size, and larger spheroidal bodies as well as rods and rarer lath-like plates. These aggregates and the original organic constituents were secreted as stratiform successions in two distinct layers, as in Recent *L. anatina*. The outer, lithified part of the primary layer bears microstructural moulds of a totally degraded periostracum and was probably composed mainly of acidic glycosaminoglycans (GAGs); the inner part evidently contained a higher proportion of spherular apatite within the GAGs than in living species. The secondary layer consists of variably complete rhythmic sets of compact, rod and plate (virgose), and membranous laminae. Compact laminae are normally cleaved along degraded walls of GAGs whereas the original GAGs-filled spaces of virgose laminae are partly occupied by recrystallized apatitic sheets with kaolinite. The phosphatized membranous laminae probably contained more spherular apatite in life than present day *Lingula*. The shell is canaliculate with chambers and galleries well developed in the virgose laminae.

There is a decrease in concentration of amino acids from the posterior to the anterior of the valves of living *Lingula anatina* and *Glottidia pyramidata* resulting from the proteinaceous coat of the apatitic spherules. A similar distribution of hydroxyproline occurs, indicative of collagen in the body platform of living lingulids. Nearly all organic constituents have been degraded in the Carboniferous valves but threads, about 50 nm thick, occasionally traverse spaces in virgose laminae and even form a network coated with spherular apatite, which resembles webs of collagens or actin found in living lingulids. Acidic and aliphatic amino acids were extracted from *L. squamiformis* valves from Calderwood and Kinghorn whereas the narrower range of amino acids from the heavily pyritized valves from Ardross confirmed differential degradation of organic material during the fossilization of penecontemporaneous samples.

The fossilization of complete shells of *L. squamiformis* is not due exclusively to catastrophic burial as has been deemed necessary to preserve Recent *Lingula* intact. The living shells of Carboniferous species were more apatitic than those of Recent *Lingula*, especially in the anteriomedian sectors of the secondary layers.

1. INTRODUCTION

The organophosphatic-shelled brachiopod *Lingula* Bruguière is the best known example among metazoans of phylogenetic conservatism. The highly characteristic shape of the streamlined, parallel-sided shell, the unique grouping of the attachment scars of the muscle system controlling the movements of the inarticulated valves and the sporadically preserved internal impressions of coelomic canals within the mantles and of the paired pedicle nerves on the ventral body platform, are all diagnostic of a continuous lineage from the Lower Palaeozoic era to the present day (figures 1–4).

Even the long muscular pedicle, which controls the position of the living animal in its burrow, has always been a salient lingulid feature judging from the extraordinary preservation, in early Cambrian mudstones, of impressions of the organ attached to *Lingulella* (Jin *et al.* 1991).

This conservatism in body form is linked with the constancy of the lingulid habitat throughout the geological record. Lingulids seem always to have lived infaunally at optimal infralittoral depths to about 20 m but frequently ranging into the intertidal zone (Paine 1970; Plaziat *et al.* 1978). The preferred substrate of living *Lingula* varies from well-sorted clay sands to coarser sands in a silty matrix. The consistencies of such sediments afford more stable burrows than exclusively clays or sands (Emig 1984, 1986), an environmental advantage which presumably exercised selective pressure during lingulid evolution.

In view of the apparent geological constancy of these environmental constraints on body form, it could be argued that the nondescript shell and those few anatomical features impressed on valve interiors may not adequately reflect the extent of change incurred during lingulid evolution. This assumption can be tested as the shell itself is chemico-structurally very complex (Williams *et al.* 1994). About one-half of the

Phil. Trans. R. Soc. Lond. B (1996) **351**, 33–49
Printed in Great Britain

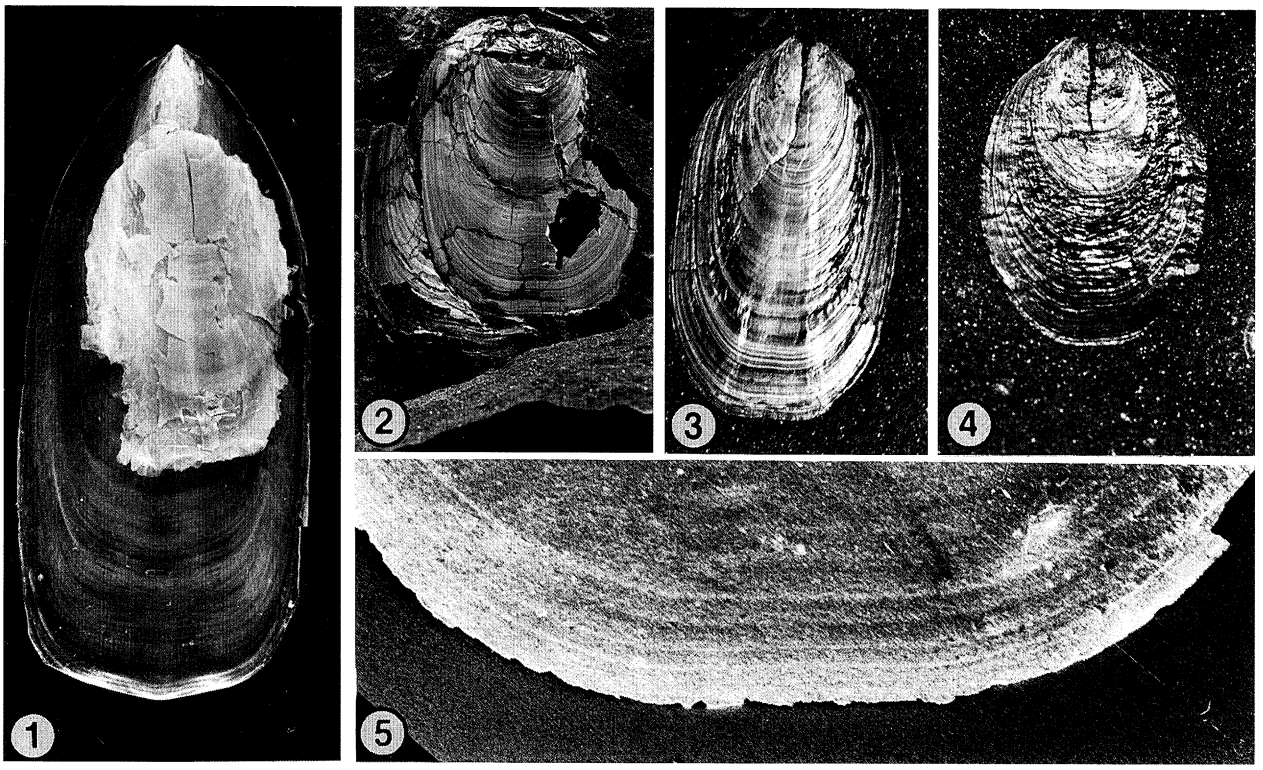

Figure 1. External view of the ventral valve of *Lingula anatina* in the background with the remains (treated with 40 % sodium hypochlorite for 24 h) of the matching dorsal valve superimposed. × 2.4 natural size.

Figure 2. Skewed valves of a complete shell of *Lingula squamiformis* from Kinghorn. × 2.1 natural size.

Figures 3 and 4. External views of dorsal valves of *Lingula squamiformis* from Calderwood showing general shape and the wrinkling of shell. × 5 and × 6 natural size, respectively.

Figure 5. SEM of the anteriomedian margin of the valve of *Lingula squamiformis* from Calderwood showing the complete phosphatization of the anterior margin. × 35 natural size.

shell dry mass is organic, consisting of glycosaminoglycans (GAGs) and β-chitin with minor fibrous collagen and at least nine other proteins. The remaining biomineral component is exclusively the fluorapatite francolite. It is secreted as organically wrapped granules about 10 nm in size, which form complex aggregates in rhythmically arranged stratiform laminations. Such a shell succession is a biochemical and ultrastructural gauge of the differentiation of the secreting outer lobe and epithelium of the *Lingula* mantle. It should, therefore, afford a finely graduated measure of the evolution of the shell, provided most components of the shell survive fossilization in a chemically or structurally identifiable state.

At first sight this prospect may seem unlikely. Fossilization of skeletal remains is allegedly accompanied by rapid degradation of all but the most durable of organic polymers. Indeed, field and laboratory observations prompted Emig (1990) to conclude that the organic component of the shell is so quickly hydrolysed or digested by microbes and the exposed apatitic framework so easily abraded hydrodynamically that fossilization of lingulid shells could only have taken place after catastrophic changes in the *post mortem* environment.

The abundance of fossil lingulid shells at palaeoenvironmentally propitious horizons throughout the geological column is indisputable. Such occurrences, however, could have resulted not only from catastrophic changes in past environments but also from chemico-structural changes in the shells themselves. Accordingly, it was decided to explore these assumptions by comparative studies of fossil lingulas. The Carboniferous successions of Scotland are famous for the richness and remarkable preservation of their fossil assemblages including beds of *Lingula* which must have accumulated in sublittoral to intertidal environments under conditions similar to those favouring living species in the warm temperate to equatorial zones of the Pacific at the present time (Craig 1952). Three samples of *Lingula squamiformis* Phillips were obtained from the Dinantian Series, to compare the chemico-structure of disarticulated and conjoined valves, which are assumed to have accumulated in different environments. The comparative chemico-structural investigations of these samples and living *Lingula* have revealed noteworthy aspects of the relative roles of various taphonomic and geological factors in shell degradation.

2. MATERIALS

The distinctive lingulid '*Lingula*' *squamiformis* Phillips has a relatively restricted stratigraphic distribution within the Carboniferous successions of the Midland Valley of Scotland (figure 6). The species is especially characteristic of the Lower Limestone and

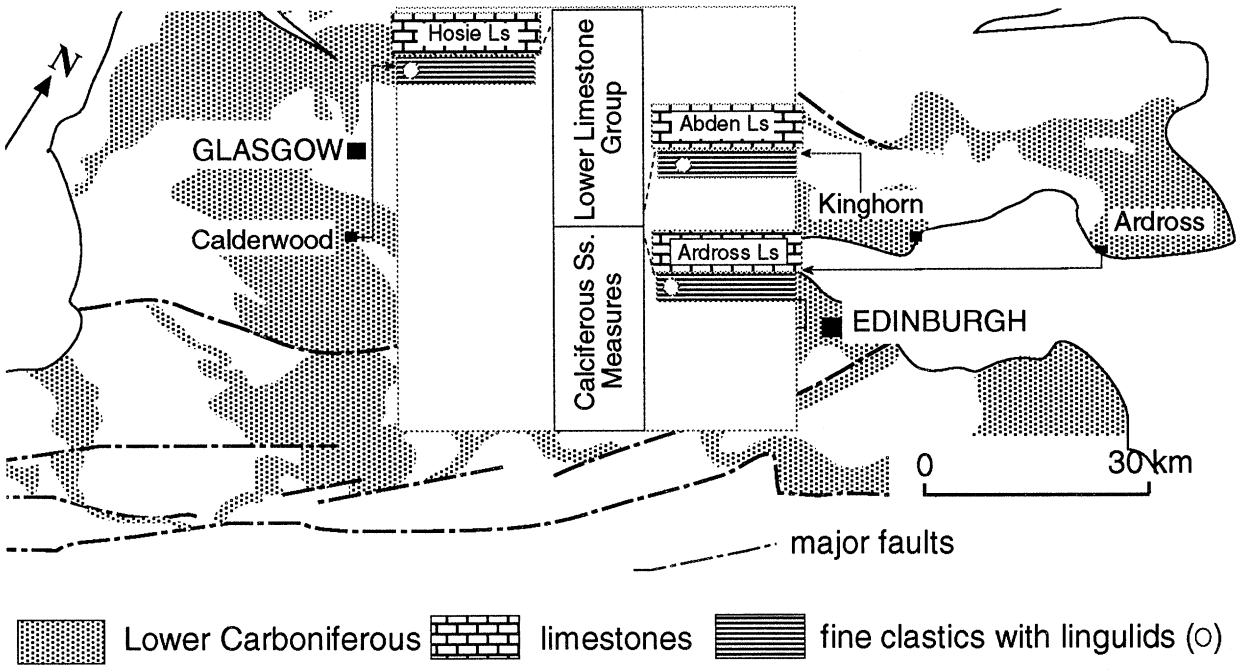

Figure 6. A map of the Lower Carboniferous rocks, exposed in the Midland Valley of Scotland, identifying the three localities yielding *Lingula squamiformis* with generalized sections showing the stratigraphic horizons of the collections relative to distinctive Dinantian limestone members.

Limestone Coal Groups and is very common at certain horizons with adult shells up to 4 cm long (Graham 1970, p. 172). The generic affiliations of the species is in doubt only in the following respect. Another genus, *Lingularia*, has been founded (Biernat & Emig 1993, p. 10) for Palaeozoic and early Mesozoic lingulas which are said to differ from more recent *Lingula*, like the living *L. anatina* Lamarck, mainly in the shape of the posterior adductor muscle scar and a proportionately longer ventral body platform. *L. squamiformis* has been meticulously described by Graham (1970, pp. 150–152) who, after an exhaustive study of all available collections, was unable to determine with certainty the full complement of muscle scars on the valve interiors let alone the variability of their distribution on the body platforms. Accordingly, we shall continue to identify the species '*squamiformis*' as *Lingula* which it is in every other morphological respect.

Three samples of *L. squamiformis* were collected from argillaceous strata associated with various carbonate members of the Lower Limestone Group and the top of the Calciferous Sandstone Measures (figure 6). The successions are cyclic with marine limestones and shales, sandstones, clay band ironstones, and rare seat earths and coals indicative of a paralic environment.

The Calderwood sample was retrieved from less than 1 m of grey shales with rare silty partings associated locally with the Top Hosie Limestone and exposed in Calder Glen near East Kilbride (N. D. L. Clark, *personal communication*). The fissility of the shales is greatly enhanced by the presence of bedding surfaces covered with disarticulated valves (figures 3 and 4), commonly entire and overlapping one another but seldom with any preferred orientation. The first 50 complete dorsal valves to be measured ranged from 1.8–21.5 mm in length with bimodal frequency peaks between 2–3 mm and 6–7 mm. This distribution probably reflected natality rates and there was little sorting of the valves other than by a sufficient drift in gently moving seawater to disengage matching valves after body decay. It is also assumed that successive *L. squamiformis* populations lived more or less *in situ* and that some catastrophic factor (Emig 1981, 1990), like periodic floods of fresh water over lagoonal flats, was responsible for the death of local populations resulting in mass expulsion of shells from their burrows (Morse 1902) and their subsequent preservation as residual fossil communities.

The second sample was collected from within the lower 3 m of a shale sequence intercalated between an underlying terrestrial seat earth and the succeeding sublittoral second Abden Limestone, which are exposed on the foreshore near Kinghorn. The shales yielding the lingulids, constitute the lower two topozones of Ferguson (1962, p. 1092) and are finely laminated with streaky lenticles of fine sand. A detailed study by Ferguson (1963) of the fossils and lithology of this transgressive sequence showed that the shells of successive populations of *L. squamiformis* varied between 1.25–25 mm in length and that about one-quarter were disposed vertically or at high angles to the bedding, effectively in the living position. Another 10% or so of the specimens lying parallel to bedding were complete shells or slightly skewed conjoined valves (figure 2); the remainder were single valves. Ferguson (1963, p. 677) noted that shells in life position (fossil census communities) were concentrated towards the base and the top of the sequence in shales that had originally accumulated as intertidal and subtidal muds respectively, according to palaeoecological evidence. Emig later concluded (1981, p. 154) that these fossil census communities in the Kinghorn sequence had

been killed by fluctuations in salinity and reductions in the particle size of the entombing sediment. In contrast, assemblages of skewed and disarticulated shells, which were characteristic of the middle part of the sequence, were similar to the residual fossil communities of Calderwood. They have been described as the remains of individuals that had flourished in optimal conditions and died through natural causes (Ferguson 1963, p. 577).

The third sample was taken from about 1 m of dark-coloured mudstones, with little discernible bedding, immediately underlying the dolostone at the base of the Ardross 'Shrimp-bed' (Cater *et al.* 1989, p. 10; Clark 1989, p. 100), exposed on the foreshore near Ardross. Here too, complete shells with the conjoined valves normally crushed, are relatively common and are inclined at various angles to the putative surfaces of deposition within the sequence. The mudstone is much less fissile than those at Calderwood and Kinghorn and shows traces of disturbed, impersistent silty laminae. These characteristics and the presence of abundant iron sulphide suggest that the Ardross *Lingula* populations were fossil census communities that had been catastrophically buried by slumping within an anoxic sludge.

The living lingulids used in this investigation were *Lingula anatina* from intertidal silts in Ariake Bay, North Kyushu, Japan, collected by A.W.; and *Glottidia pyramidata* (Stimpson) from sandbars in Florida, U.S.A., purchased from the Gulf Specimen Company Inc.

3. METHODS

The procedures followed for preparing living material for examination under electron microscopes (including enzymic digestion of sections) are fully described by Williams *et al.* (1994), pp. 262–266, and are therefore not repeated here. The preparation of fossils is almost the same as that for living shells. Fracture sections (preferably with adherent matrix) and valves surfaces were cleaned of most extraneous particles by an air jet or exceptionally by brief sonication in acetone before coating with gold or carbon, dependant on whether the specimens were being scanned for structural detail or energy dispersive spectrometer (EDS) analysis.

For amino acid analysis of living valves, body tissue was removed and the valves cleaned by abrasion with fine sandpaper. Sonication was used to remove loosened material. Cleaned valves were cut transversely into four parts which were then ground in liquid nitrogen using a pestle and mortar. Valve powders were dissolved in HCl (2N) to a ratio of 11 μl per mg shell. Aliquots were hydrolysed manually before loading onto a 420 amino acid analyser from Applied Biosystems to determine the total levels of (both peptide-bound and free) amino acids. Fractions were also loaded directly onto the analyser without hydrolysis to determine the level of free amino acids present. Aliquots from each of the four valve portions were pooled to determine the amino acid composition of the entire shell. For manual hydrolysis, vials containing 500 μl of HCl (6N) were purged with argon at 2–3 psi for 30 sec. Lyophilized samples in hydrolysis tubes were placed in the hydrolysis vials, each sample purged with nitrogen, vials closed and vapour-phase hydrolysis carried out by incubation at 165 °C for 1 h. Hydrolysed samples were then reconstituted in an aqueous solution of EDTA (0.005%). Amino acid analysis of fossils followed the same procedures and samples of the entombing sediments were also analysed to enable identification of any homogenization in amino acid profile between the shell and the matrix. Values for amino acid analysis of living valves are for peptide-bound amino acids whereas for fossil samples, values obtained with and without hydrolysis are presented.

4. RESULTS

The shells of Carboniferous lingulids, like those of living species, are organophosphatic. However, the organic content has been reduced to traces of a relatively few polymers; and even the fluorapatitic constituents have usually undergone some recrystallization. Yet both fossil and living biomineral textures are similar in that the smallest, discrete phosphatic particles found in Carboniferous shells, are between 20–60 nm in size (figures 14, 18 and 34) and are indistinguishable from the spherules of Recent shells. Indeed, in especially well preserved fossils, it is evident that these spherular bodies are also aggregates,

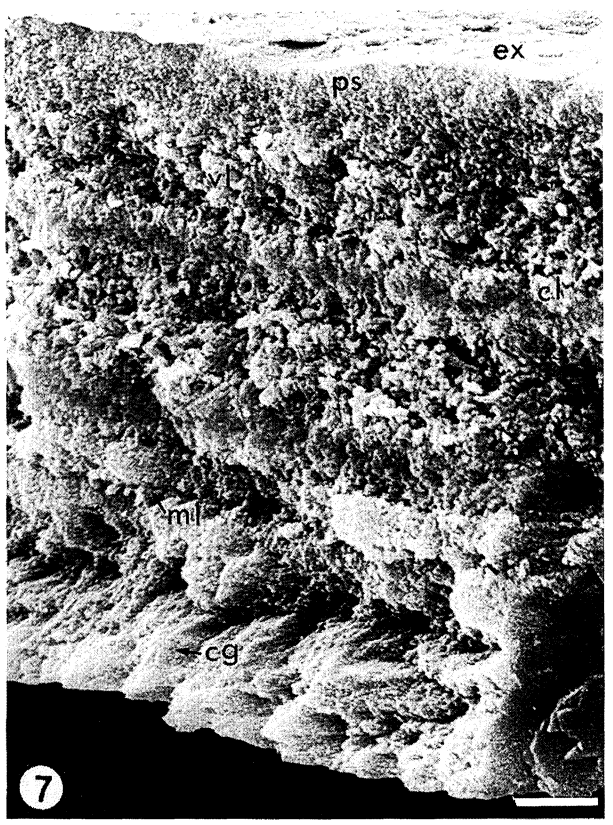

Figure 7. SEM of a gold-coated vertical fracture section of a valve of *L. squamiformis* from Calderwood showing the general succession of primary shell (ps) at the external surface (ex) underlain by sets of membranous (ml), compact (cl) and virgose (vl) laminae, affected by vertical cleavage (cg). Scale bar = 2 μm.

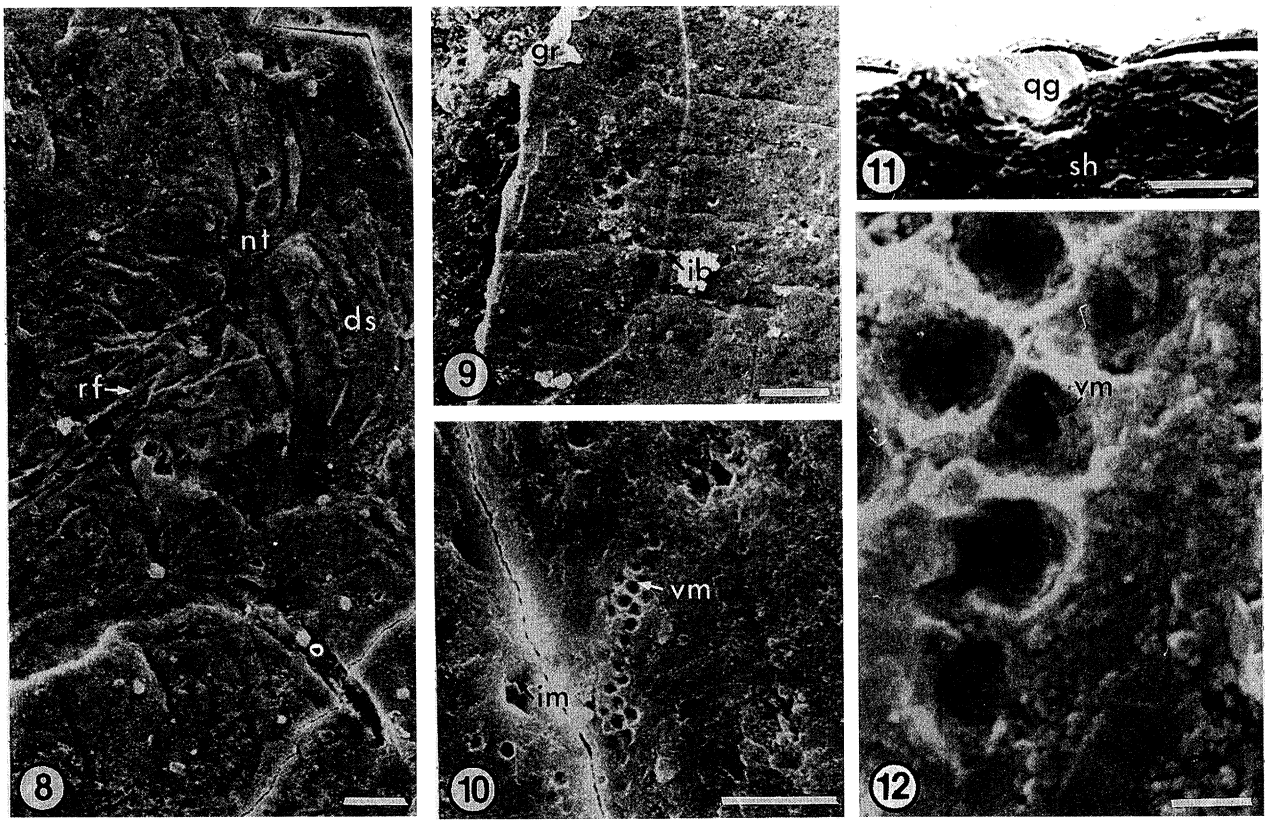

Figures 8–12. SEMs of gold-coated external surfaces and one fracture section of valves of *L. squamiformis* from Calderwood.

Figure 8. Surface deformed by drapes (ds) and nickpoints (nt), and radial folds (rf). Scale bar = 10 μm.

Figure 9. Moulds (ib) of thickened intercellular deposits defining vesicular cells orthogonal to a growth edge (gr). Scale bar = 25 μm.

Figures 10 and 12. General view and detail of moulds (vm) of a close packed raft of vesicles, with impact moulds (im) of coarser clastic grains in entombing sediment. Scale bars = 5 μm and 500 nm, respectively.

Figure 11. Fracture section showing a valve as a thin sinuous band bending around a quartz grain (qg) in the shale (sh). Scale bar = 100 μm .

presumably of apatitic granules, up to 10 nm in size, the basic biomineral component of *Lingula* (Williams *et al.* 1994).

The spherules are themselves aggregated into larger bodies of varying intricacy, which in turn are assembled into stratiform laminae (figures 7 and 17). Such successions are so like those secreted by the living mantle that it is appropriate to discuss them in the same order and with the same terminology as were adopted to describe the shell of living *Lingula anatina* (Williams *et al.* 1994).

The most plentiful sample of *L. squamiformis* at our disposal was that from Calderwood. It was, therefore, chosen as the standard by which the variability of the chemico-structure of lingulid shells in the Carboniferous successions of Scotland was measured. Comparisons have been drawn continually with Recent lingulas as represented by the Pacific *L. anatina*; and this specific name has been used to identify the living comparator.

(*a*) *General structural features of the shell*

The shell of *L. squamiformis* is extremely thin even in comparison with that of living species like *L. anatina* which, at maturity, is seldom more than 1mm posteriomedianly (figure 7). Valves from Calderwood, between 6–10 mm long, are normally less than 100 μm thick thinning to 20 μm laterally. Indeed only some Kinghorn shells were more robust, with one dorsal valve just over 200 μm thick posteriomedianly and 60 μm laterally although it was about 25 mm long. The shells were also very flexible as is indicated by the small scale wrinkling of valves usually as transverse corrugations with wavelengths of 200 μm or so (figure 4). This *post mortem* folding arose during compaction of the sediments which also induced, without fracture, sharp flexures around coarse particles in the matrix (figure 11) without fracturing the shell except along the line of the dorsal median septum (figures 3 and 4).

(*b*) *Shell surface*

The external surface of the shell of the Calderwood *L. squamiformis* is normally rich in original microtopographic features. Differentially coloured growth banding, at intervals of about 50 μm along the anteriomedian vector, serves as a concentric grid in determining the nature and attitude of finer structures. The most common of these are sets of folds (13 μm in

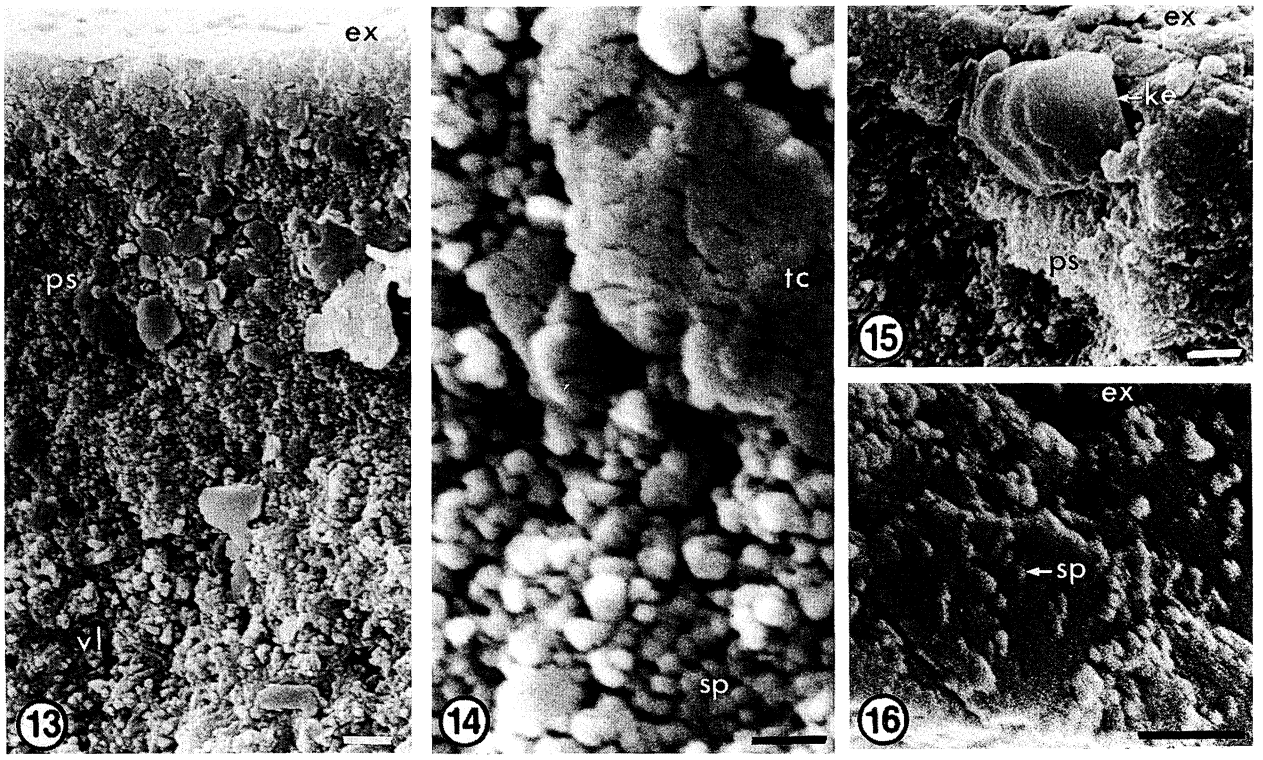

Figures 13–16. SEMs of gold-coated vertical fracture sections of valves of *L. squamiformis* from Calderwood.

Figures 13 and 14. General view and detail of primary layer (ps), forming the external surface (ex) and succeeded by a virgose lamina (vl), with dehydrated recrystallized patches of tension-cracked (tc) apatite with clay and spherular apatite (sp) surviving more or less intact. Scale bars = 1 μm and 250 nm, respectively.

Figure 15. Primary layer (ps) immediately below the external surface (ex) of a valve containing a book of kaolinite (ke). Scale bar = 1 μm.

Figure 16. Primary layer immediately below the external surface consisting of recrystallized pinacoids of apatite with kaolinite traces, partly incorporating apatitic spherules (sp). Scale bar = 1 μm.

wavelength), disposed as outwardly convex arcs (drapes) subtending re-entrant angles with radial tracks (nickpoints) which may be up to 75 μm wide and 400 μm long (figure 8). These structures are identical with those formed by stress couples, set up in the marginally expanding periostracum and primary layer of living *Lingula* during their secretion and migration relative to the underlying outer mantle lobe. Second order radial (figure 8) and transverse periclinal folding with wavelengths of 1.5 μm, superimposed on drapes, also occur and are identical with those found in *L. anatina* especially along the marginal folds. Other features, not found in the living shell, include parallel grooves about 9 μm apart, lying orthogonal to growth margins (figure 9) and clusters of close-packed hemispherical depressions up to 50 nm in diameter (figures 10 and 12). These are interpreted as having become exposed during the *post mortem* degradation of the periostracum as they are likely to be respectively: traces of the intercellular boundaries between the elongated vesicular cells of the outer mantle lobe; and groups of exuded vesicles trapped like incipient bubble rafts between the periostracum and primary layer.

Sporadically occurring, sharp-angled indentations are impressions made by crystalline grains in a compacting sediment (figure 10). The surfaces bearing these microstructures are usually kaolinized but never completely enough to mask the presence of apatitic spherules about 40 nm in size (figure 12) which may coalesce into elliptical pads up to 300 nm across rather like two dimensional mosaics.

The external surfaces of *L. squamiformis* shells from Kinghorn and Ardross are also kaolinized and spherular with well developed microtopographic features especially drapes and nickpoints.

(*c*) *Primary layer*

As in living lingulids, the primary layer of *L. squamiformis* is easily distinguishable in the relative constancy of its thickness and the uniformity of its texture (figures 7 amd 13). The average thickness of the layer in the Calderwood sample, at just over 4 μm, was greater than those of the Kinghorn and Ardross shells (3 μm) but very much less than a mean of 40 μm estimated for a mature *L. anatina*, more than 30 mm long (Williams *et al.* 1994, p. 241). The thickness of this layer can increase incrementally with shell growth but not to such an extent as to invalidate the conclusion that the primary layer of the Carboniferous *Lingula* was significantly thinner than in living species.

The texture and composition of the fossilized primary layer of *L. squamiformis* is necessarily different from that of *L. anatina* which is composed mainly of acidic GAGs and minor apatite commonly in stratified

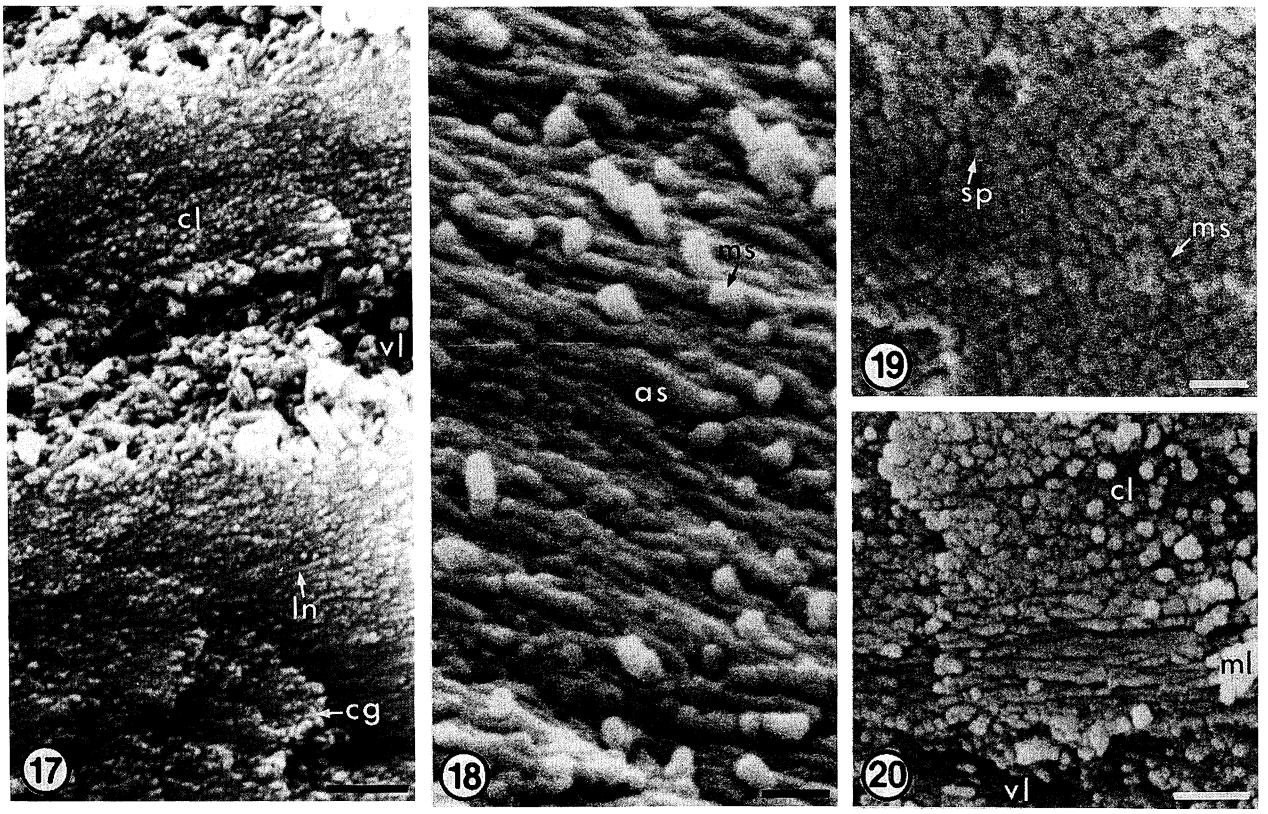

Figures 17–20. SEMs of gold-coated vertical fracture sections and an internal surface (figure 19) of valves of *L. squamiformis* from Calderwood.

Figure 17. Compact laminae (cl), interleaved with virgose laminae (vl), showing lineation (ln) and cleavage (cg). Scale bar = 1 μm.

Figure 18. Detail of a lineated compact lamina composed of 'worm-like' arrays of spherules (as) and larger mosaics (ms). Scale bar = 250 nm.

Figure 19. External surface view of a compact lamina showing the range of granular aggregates from spherules (sp) to mosaics (ms). Scale bar = 250 nm.

Figure 20. Recrystallized membranous lamina (ml) intercalated between the base of a compact lamina (cl) and the top of a virgose lamina (vl). Scale bar = 500 nm.

lamination. There is, moreover, a much higher proportion of spherular apatite, usually aligned like strings of beads up to 1.2 μm long in compact laminae but also aggregated into mosaics, up to 400 nm in size, clustered in highly inclined walls separated by recrystallized sheets of apatite with traces of kaolinite (figures 14–16).

The recrystallization of the primary layer is variable within and between samples. The Ardross specimens appear to have suffered more kaolinization and apatitic recrystallization than the Kinghorn and Calderwood shells.

(*d*) *Secondary layer*

The secondary layer of *L. squamiformis* is similar to that of *L. anatina* in the variable thickness of its stratiform succession of laminae (figure 7). The succession, which is essentially rhythmic (figures 17 and 22), is thickest posteriomedianly and its marginal attenuation involves the thinning out of laminae, their lateral passage from one kind to another and their overstep by younger, inner unit(s). This complex vertical and lateral sequence is decipherable because the laminar constituents retain their distinctiveness over relatively large areas and will be described before the nature of the succession is discussed.

(*i*) *Compact laminae*

The compact laminae of Carboniferous lingulas are as easily recognized as they are in Recent *L. anatina*. In the *L. squamiformis* shells from Calderwood, the compact laminae have a mean thickness of 4 μm, compared with 4 μm and 3.5 μm for the Ardross and Kinghorn samples respectively (and 3.2 μm for *L. anatina*); although thicknesses vary from less than 1 μm to 21 μm posteriomedianly.

A typical lamina consists of well compacted aggregates of apatitic granules varying from spherules and mosaics to larger botryoids (figures 17–20). Worm-like arrays of spherules, up to 1.5 μm long are common and impose a vertical as well as a horizontal lineation on the lamina (figure 18). This widespread alignment is interpreted as an epitaxial layering induced by the secretion of spherules along ordered chitinous fibrils. In addition, the compact laminae of *L. squamiformis* are vertically cleaved (figures 7 and 17) at intervals of

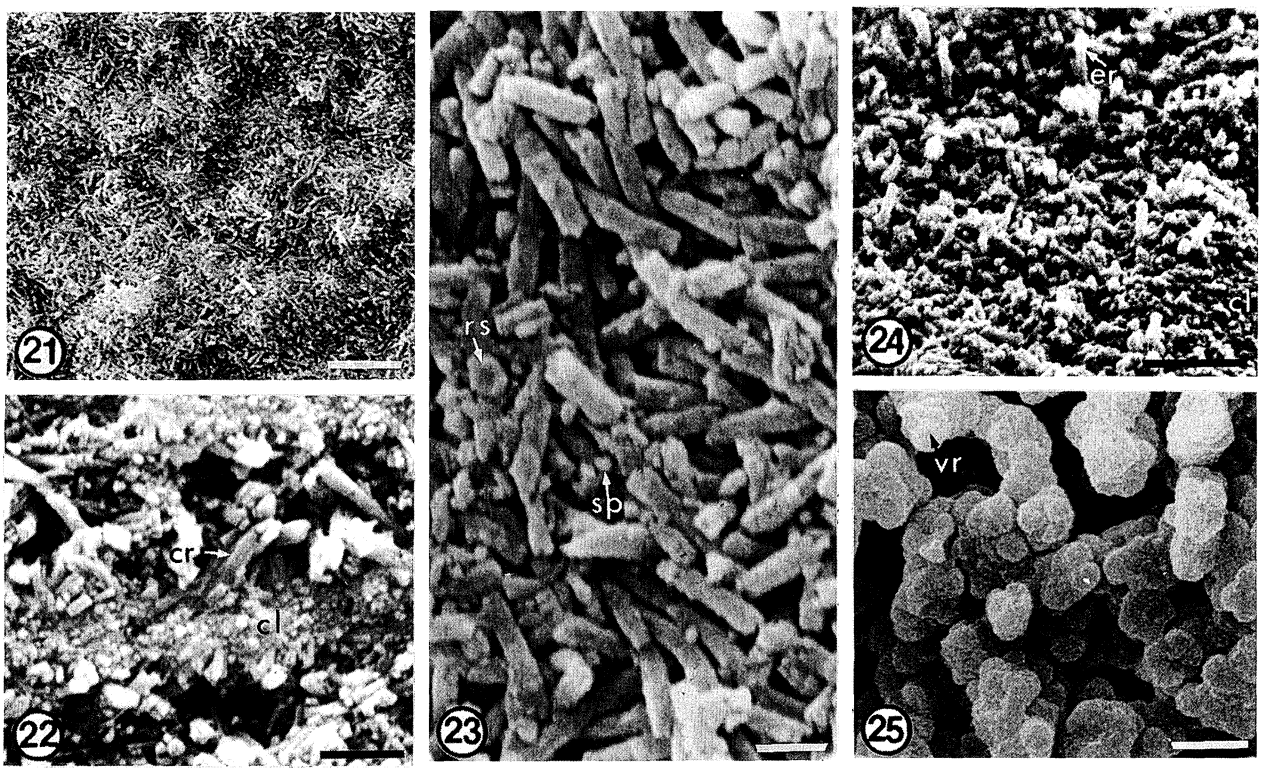

Figures 21–25. SEMs of various gold-coated surfaces of valves of *L. squamiformis* from Kinghorn and Calderwood (figures 22 and 24).

Figures 21 and 23. External view and detail of a virgose lamina with rods distributed as low mounds separated by shallow troughs reflecting the microtopography of the secreting plasmalemmas of the outer epithelium; the ring-like arrangement (rs) of spherules is seen in transverse sections of some rods and scattered isolated spherules (sp). Scale bars = 5 μm and 500 nm respectively.

Figure 22. Vertical fracture section of a compact lamina (cl) developed between two thin laminae of rods some of which are curved (cr). Scale bar = 1 μm.

Figure 24. Oblique view of the base of a virgose lamina succeeding a spherular compact lamina (cl) and including some erect rods (er). Scale bar = 1 μm.

Figure 25. External view of a virgose laminae with coalescing vertical rods (vr) and scattered spherules forming a labyrinth. Scale bar = 2 μm .

between 4–5 μm, which is also present in the *L. anatina* shell where it corresponds to sheets of GAGs partitioning the apatitic components.

Compact laminae are least affected by recrystallization, presumably because of the close packing of the biomineral components during secretion. When recrystallization did take place, it normally gave rise to arrays of acicular prisms, up to 1 μm long, disposed orthogonally to the bounding surfaces of compact laminae. The prisms were prone to develop at the interface between compact and virgose laminae. The occurrence of spherules partly incorporated within such prismatic arrays suggests that the crystals are transformations of rods originally disposed at high angles to the interface. This is the alignment of well preserved rods in sections unaffected by recrystallization (figure 24). Similarly, recrystallization within compact laminae tended to result in prisms more or less parallel with the lineation of spherules.

(ii) Virgose (rod and plate) laminae

The compact laminae of the shell of Carboniferous *Lingula* are almost invariably succeeded by more dispersed aggregations of apatitic spherules in the form of cylindroids, laths, plates, mosaics and botryoids. These open successions are distinctive stratiform units which, on average, are 4.2 μm thick in the Calderwood shell compared with 4.5 μm and 6.6 μm in the Kinghorn and Ardross samples respectively and may exceptionally exceed 20 μm. The units are homologues of the 'rod and plate laminae' of *L. anatina*, which *in vivo* are impregnated with GAGs; for convenience they are described as virgose (*virgosus* L. 'full of twigs').

The most conspicuous constituents of these laminae are apatitic cylindroids, up to approximately 1.7 μm long and about 250 nm thick (figures 21–25). The rods are composed of spherules, about 40 nm in size, which are closely packed superficially but without any discernible stacking pattern. Transverse fracture sections of some rods bear central depressions and look like rings of five or six spherules, about 200 nm in diameter, which are sparsely scattered throughout the laminae (figure 23). The possibility that the rods were formed by spherules aggregated around organic axes is supported by several characteristics of the rods. These include: the curved or sinuous attitudes and uniform thicknesses of many discrete rods (figure 22); their occurrence and position of growth, as pillars arising

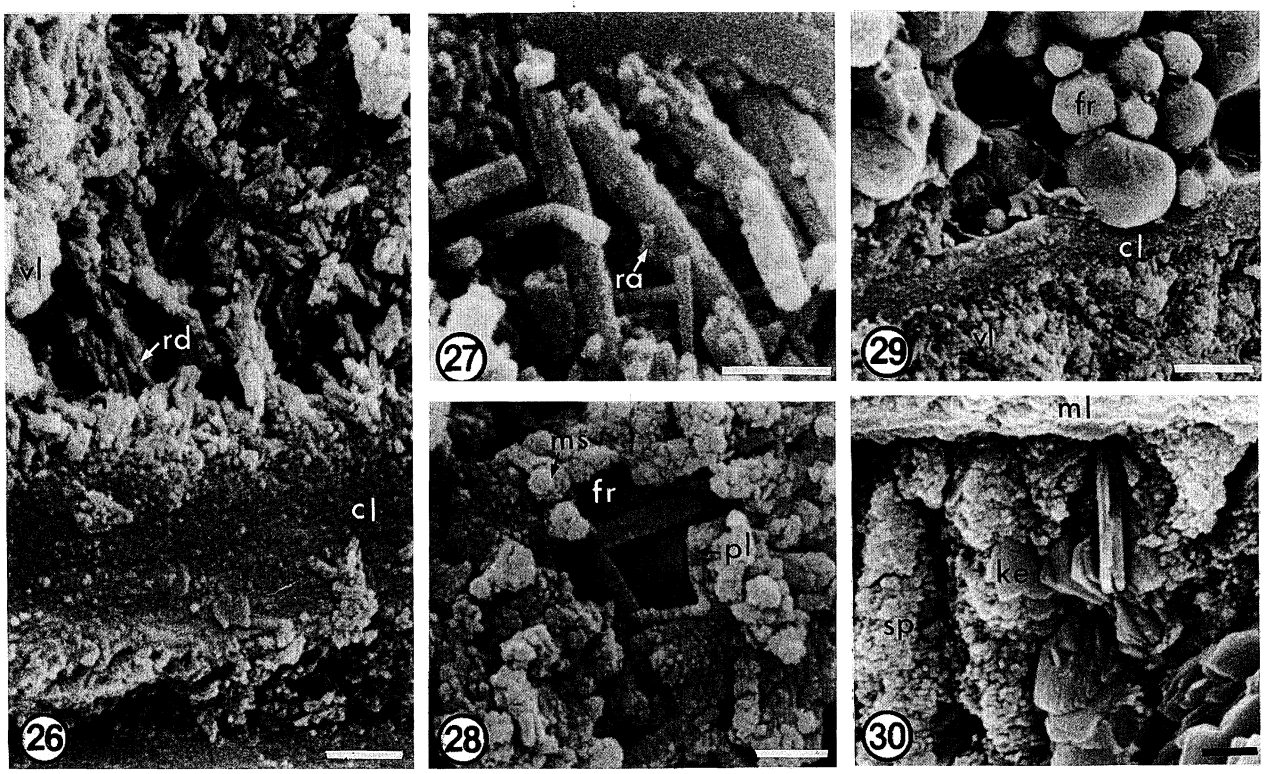

Figures 26–30. SEMs of gold-coated vertical fracture sections of *L. squamiformis* from Calderwood, Kinghorn (figure 28) and Ardross (figure 30).

Figure 26. A virgose lamina (vl) with recrystallized rods (rd) and sparse spherules marking the transition from the underlying compact lamina (cl) composed of spherules and mosaics and containing some recrystallized rods arranged in a lattice. Scale bar = 1 μm.

Figure 27. Recrystallized rods of a virgose lamina, some with superficial second order prisms (ra). Scale bar = 500 nm.

Figure 28. Differentially recrystallized virgose lamina with partly intergrown (pl) clusters of spherular mosaics (ms) and recrystallized prismatic plates engirdling a framboid (fr). Scale bar = 500 nm.

Figure 29. The interface between the matrix of a complete shell, consisting of framboids (fr) cemented by an iron-rich smectite and a recrystallized inner set of compact (cl) and virgose (vl) laminae of the secondary layer of a valve. Scale bar = 5 μm.

Figure 30. Kaolinitic plates (ke) replacing GAGs to form walls alternating with partitions of spherular apatite (sp) within a membranous lamina (ml). Scale bar = 1 μm.

from substrates of compact laminae (figure 24); and their rare assembly into regular lattices subtended at about 60° to associated compact laminae (figure 26). The loci of growth on a spherular substrate can be densely distributed with 20 or more rods occurring within the imprint of the intercellular boundary delineating a typical secretory outer epithelial cell about 7 μm across (figure 21). Traces of axial threads within apatitic cylindroids have been found in only one well-preserved complete shell from Kinghorn (figure 37). The nature of these threads is discussed in § 4(*d*) (iv).

The other constituents of virgose laminae are spherules in discrete clusters or aggregated into rings, mosaics, botryoids and rarer plates (figure 34). It is evident that all such structures as well as the cylindroids must have been suspended within GAGs in the living shell as they are in *L. anatina*. Yet the degradation of the GAGs did not result in any significant collapse or indeed much disturbance of the original biomineralized structures, suggesting that they formed traceries *in vivo* with the larger constituents interconnected by organic strands and strings of spherules.

Some recrystallization of these laminae has usually taken place both within the spaces originally filled by GAGs and of the biomineralized traceries. The replacements of GAGs normally consist of pinacoidal plates of apatite (with traces of silica and alumina) and, more rarely, books or separate leaves of kaolinite (figures 26, 27 and 30); partly incorporated spherules can be found in both kinds of plates (figure 28). Framboidal pyrite also occurs as discrete spheroids up to 7 μm in diameter and are commoner in the Ardross shells (compare figure 29) than in those from Calderwood and Kinghorn (figure 28). Recrystallization of the original organophosphatic bodies is mainly by 'pseudomorphous' replacement (figures 27 and 28). Groups of cylindroids, for example, may be replaced by several generations of prismatic apatite which together mimic the curved dispositions and thicknesses of original bodies. In a like manner, mosaics may be replaced by spherulites composed of acicular apatite.

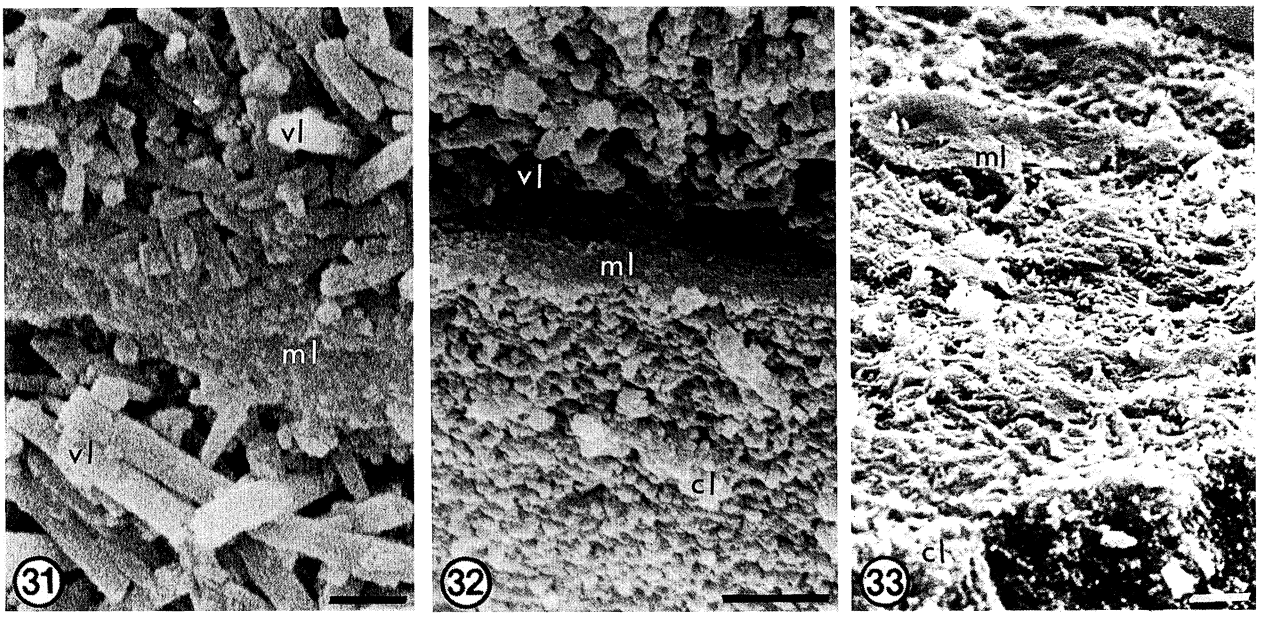

Figures 31–33. SEMs of vertical and oblique fracture sections of membranous laminae in the secondary layers of valves of *L. squamiformis* from Kinghorn and Calderwood (figure 33).

Figure 31. Phosphatized membranous lamina (ml) between two virgose laminae (vl). Scale bar = 500 nm.

Figure 32. Phosphatized membranous lamina (ml) between compact (cl) and virgose (vl) laminae. Scale bar = 1 μm.

Figure 33. Oblique view of the external surface of a compact lamina (cl) with adherent fragments of a lithified membranous lamina (ml). Scale bar = 1 μm.

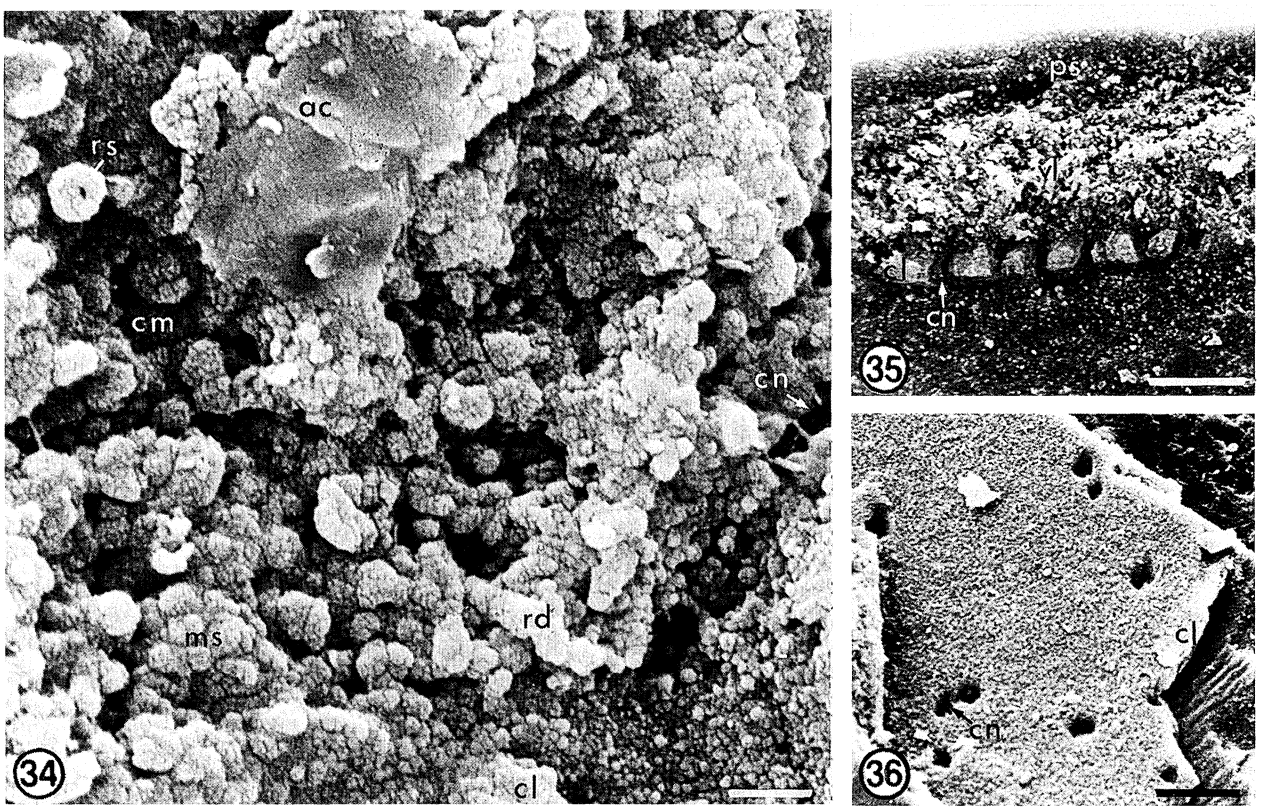

Figures 34–36. SEMs of gold-coated vertical and oblique fracture sections of valves of *L. squamiformis* from Kinghorn (figure 34) and Calderwood.

Figure 34. Details of a virgose lamina succeeding a compact lamina (cl) showing a canal (cn) traversed by an 'organic' strand, rods (rd), mosaics (ms), rings of spherular apatite (rs), a sheet of recrystallized apatite with clay traces (ac) and a chamber (cm). Scale bar = 1 μm.

Figure 35. A compact lamina (cl) perforated by canals (cn) and underlying the standard outer succession of primary layer (ps) and a virgose lamina (vl). Scale bar = 5 μm.

Figure 36. The external surface of a compact lamina (cl) perforated by canals (cn). Scale bar = 10 μm.

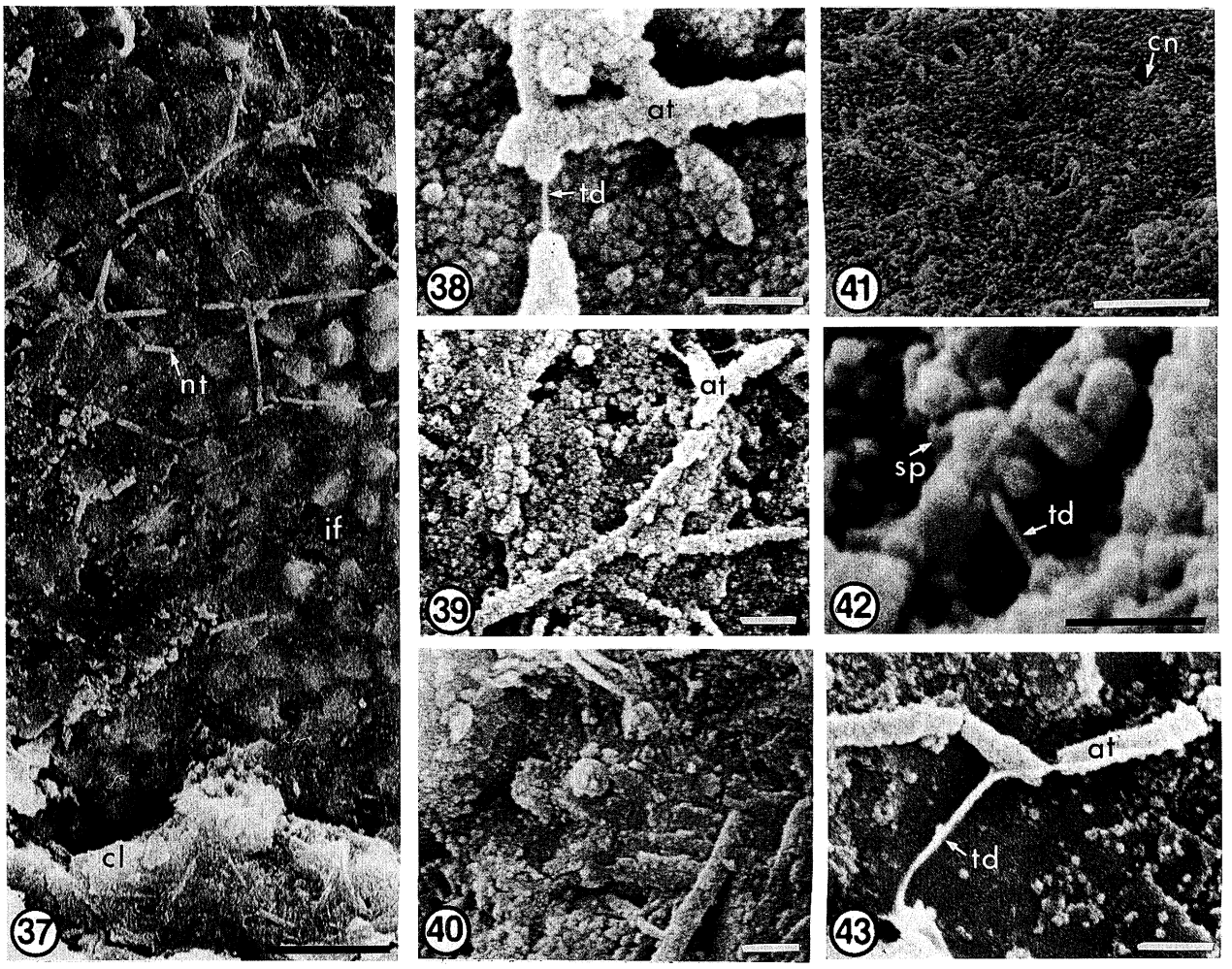

Figures 37–43. SEMs of gold-coated surfaces exposed in an oblique fracture section of the secondary layer of the valve of *L. squamiformis* from Kinghorn.

Figure 37. The external view of the interface between a matrix of illite and framboids (if) with adherent traces of a network of rods (nt) and the innermost compact lamina (cl). Scale bar = 5 μm.

Figures 38, 39 and 43. Details of the network of rods showing the nature of the spherular apatitic coats (at) encasing threads (td) presumably of organic origin. Scale bars = all at 500 nm.

Figure 40. Detail of the external surface of the compact layer seen at the bottom of figure 37, showing rods similar to those forming the network in figure 37. Scale bar = 500 nm.

Figures 41 and 42. General external view and detail of the canaliculate (cn) interface between a compact and virgose laminae showing spherules (sp) forming incipient rods and 'organic' threads (td). Scale bars = 5 μm and 500 nm, respectively.

(*iii*) *Other laminae*

Another kind of lamina which is invariably present in the *L. squamiformis* shell is a thin but widespread sequence of up to six layers, each about 150 nm thick (figures 31–33). This lamina is normally associated with a slit-like gap parallel with the stratiform succession and is interpreted as a series of lithified membranes. In living *L. anatina*, such membranes consist of layers of GAGs interleaved with proteinaceous sheets. The Carboniferous correlatives have been lithified by phosphatization as well as kaolinization, which suggests that some of the membranes were coated with monolayers of spherules as in stratified laminae of *L. anatina*.

In a few Calderwood valves, there are localized patches of near vertical pinacoidal sheets of recrystallized apatite with clay traces alternating at intervals of about 4–5 μm with walls of spherules in varying degrees of compaction (compare figures 13, 14 and 16). The apatitic sheets are interpreted as replacements of GAGs partitions in the walled laminae found in *L. anatina*.

(*iv*) *Other microstructures*

The *L. squamiformis* shell is canaliculate in the typical lingulid fashion (figures 34–36). The canals, which branch and are therefore unevenly distributed (up to 13 μm apart), can be traced continuously through two or more consecutive laminae. They are usually between 300–500 nm in diameter but dilate into galleries and chambers up to several μm in size, especially in virgose laminae. They are usually well delineated by walls studded with spherules, and in one section of a

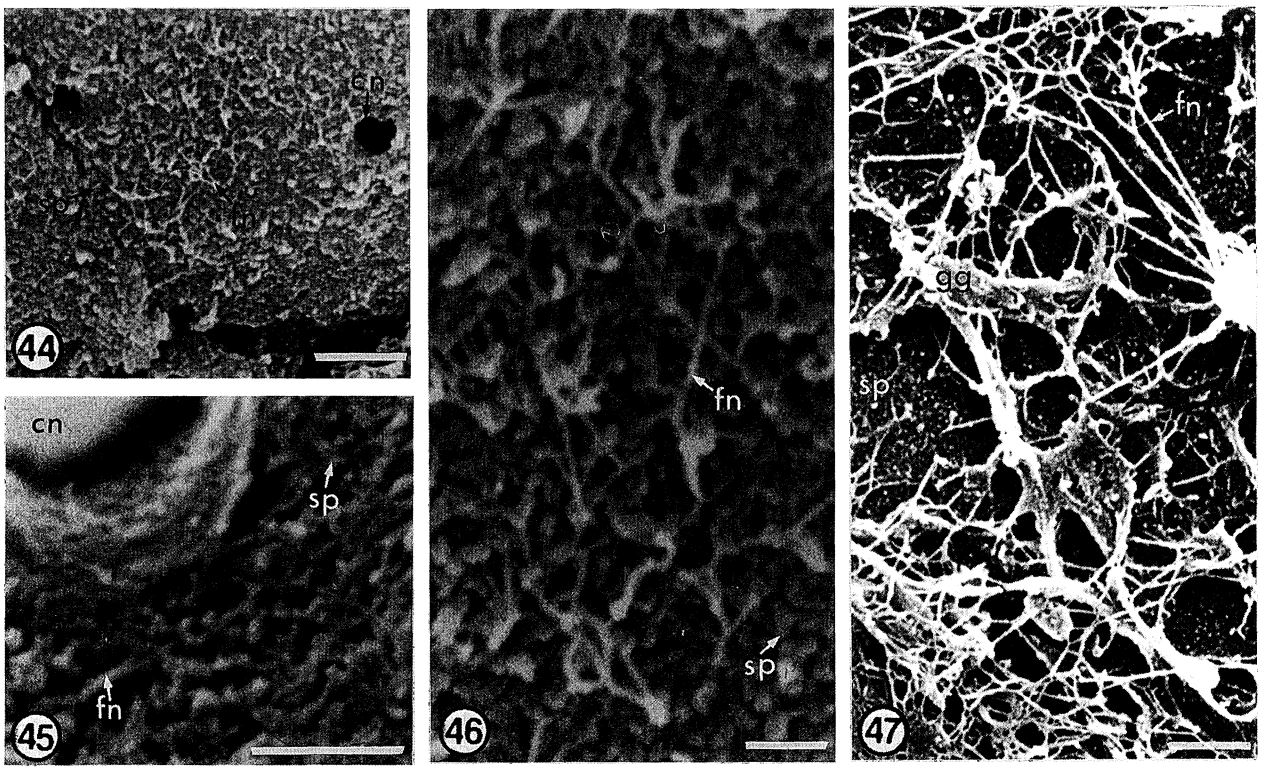

Figures 44–47. SEM of a filamentous network, interpreted as traces of the cell cortex within the shell successions of *Glottidia pyramidata* and *Lingula anatina* (figure 47).

Figures 44–46. Views of the interface between an inner membranous lamina and an outer virgose lamina, in a cut posteriomedian section of a dorsal valve digested in proteinase-k, showing a filamentous network (fn) in relation to canals (cn) and spherular apatite (sp). Scale bars = 1 μm, 500 nm and 250 nm respectively.

Figure 47. A filamentous network (fn) with some GAGs (gg) on a substrate of spherular apatite (sp) exposed below exfoliated periostracum and primary layer in the median part of the external surface of a critical point dried valve previously stored in ethanol (70% by volume). Scale bar = 1 μm.

Kinghorn shell, a canal is traversed by a few strands (40–50 nm thick) (figure 34) in the manner characteristic of *L. anatina* perforations.

The Kinghorn shell is indeed remarkable for its well preserved biomineralized microstructures which closely match their living homologues exposed by enzymic digestion of the GAGs pervading *L. anatina* shells. The strands, which are up to 500 nm long, not only cross canals but occasionally also connect adjacent botryoidal masses found within a virgose lamina in the posterio-median section where the shell is over 200 μm thick (figures 34 and 42).

Another, more anterior, piece of Kinghorn shell with adherent internal matrix was broken obliquely and mounted flat on its internal surface in order to view exposed strips of different laminae throughout the succession. On the innermost surface, representing the interface between the internal surface of the valve and the sedimentary matrix of blades of illite and framboids of pyrite, there was a network of cylindroids (figures 37–40 and 43). These microstructures were indistinguishable from others found in a virgose lamina immediately external to the network-bearing interface except for the length and branching habits of the cylindroid net. The cylindroids at both horizons consisted of close-packed spherules, between 35–60 nm in size, forming regular rods with an average thickness of 260 nm (figures 38 and 39). The rods at the interface were up to 12.5 μm long and branched at acute angles although a few were superimposed on one another more or less rectilinearly. Sporadic fractures of the longer rods exposed a thread-like core between 35–50 nm thick (figures 38 and 43). There is little doubt that all such rods, at the internal surface and within the innermost complete virgose lamina of the valve, had axial cores of threads which, in one exposure, branched successively within 500 nm at about 60° and 45°.

The lateral branching of these threads and their encasement in spherular apatite precludes an illite/smectite origin. On the other hand, they closely resemble nets of collagen or actin, sporadically associated with the membranous laminae of living *Lingula* (figure 47) and *Glottidia* (figures 44–46).

(*v*) *Laminar sets*

As in *L. anatina*, the laminae of the *L. squamiformis* shell usually group into rhythmic sets (figures 7, 17, 22 and 31). The primary layer is succeeded by a compact lamina passing inwardly into a virgose lamina (averaging 5.7 μm in the Calderwood sample) and a membranous lamina. Thereafter, this cycle – compact, virgose and membranous laminae – may be repeated several times, dependant on the size of shell and the completeness of the secretory cycle as a lamina may be poorly developed or entirely suppressed by lateral

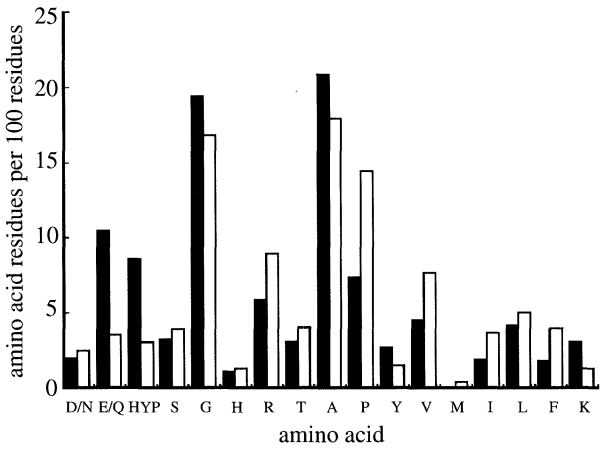

Figure 48. Amino acid composition of the valves of *Lingula anatina* (open bars) and *Glottidia pyramidata* (filled bars). Values of peptide-bound amino acids are expressed as residues per 100 amino acids to enable comparison of the amino acid profiles of *L. anatina* and *G. pyramidata* despite differences in amino acid concentration between the two genera.

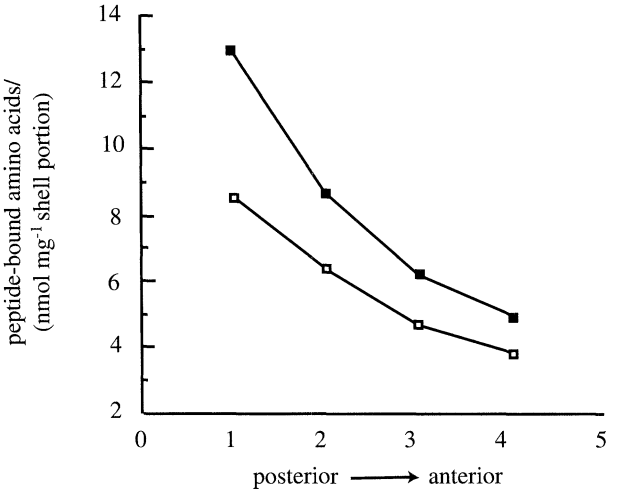

Figure 49. Distribution of amino acids in the valves of *Lingula anatina* (open squares) and *Glottidia pyramidata* (filled squares). Total peptide-bound amino acids are expressed as nmoles amino acid per mg shell for *L. anatina* and *G. pyramidata* as determined by analysis of four valve portions from the posterior to the anterior of the valve.

passage into another kind. There is also considerable variation in the thicknesses of fully developed cycles. In the Calderwood valves, these averaged 6.9–8.3 μm medianly and just over 4 μm laterally. In the largest valve (more than 20 mm long) of the Kinghorn sample, the average cycle varied from a maximum of 17 μm posterio-medianly to 13 μm or less anteriorly and laterally. These last estimates are still less than those of the average laminar cycle of *L. anatina*, which difference is only partly attributable to the intercalation of a zone of botryoids between the compact and rod and plate laminae of the living species.

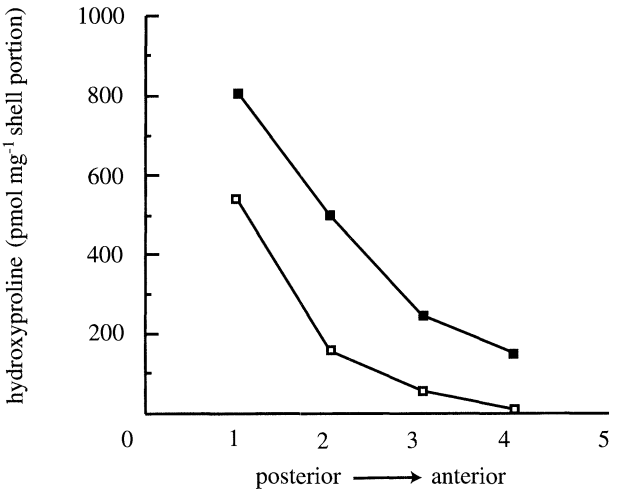

Figure 50. Distribution of hydroxyproline in the valves of *Lingula anatina* (open squares) and *Glottidia pyramidata* (filled squares). Peptide-bound hydroxyproline expressed as pmoles hydroxyproline per mg shell from the posterior to the anterior of the valve.

(*e*) *Amino acids in lingulid shells*

(*i*) *Recent shells*

The concentration of amino acids in the shell of *L. anatina* (5.8 nmole per mg shell) is lower than in that of *Glottidia pyramidata* (8.75 nmole per mg shell). Additionally, there is also a difference in the amino acid profile between the two genera with *G. pyramidata* containing higher relative levels of glutamine/glutamic acid, hydroxyproline, glycine, alanine and lysine whereas *L. anatina* contains higher relative levels of arginine, proline, valine and phenylalanine (figure 48). Despite the differences in amino acid concentration and profile, both species show a similar pattern in the distribution of amino acids throughout the shell in that there is a decrease in the level of amino acids from the posterior to the anterior of valves (figure 49). In particular, the amino acid hydroxyproline, which is indicative of the fibrous protein collagen, is present in higher levels in the posterior portion of a valve (figure 50). Among the complex mixture of proteins extracted from *L. anatina* valves, one protein has a molecular mass of 36 kDa as estimated by gel electrophoresis under denaturing conditions (Williams *et al.* 1994). Muscle actin contains 375 amino acids (Vandekerckhove & Weber 1979) which would result in a molecular weight around 40 kDa. Therefore, 36 kDa is within the calculable range for the molecular mass of the globular actins. Pending further investigations, this molecular mass has been attributed to the fibrillar webs found in Recent lingulids (figure 44–47).

(*ii*) *Carboniferous shells*

The amino acid profiles of the valves of *L. squamiformis* and their matrices show different profiles (table 1). Kinghorn and Calderwood samples contain the largest range of amino acids whereas the Ardross samples contain only glutamine/glutamic acid and glycine. Kinghorn and Calderwood samples contain the acidic amino acids or their amine form, aspartic

Table 1. *Amino acid profiles of Carboniferous lingulid valves and their surrounding sediments from three different burial environments*

(Values are expressed as pmoles amino acid per mg sample. Amino acids released with and without hydrolysis of peptide bonds are presented.)

		amino acid					
	hydrolysis	D/N	E/Q	G	A	Y	V
Kinghorn							
shell	+	5.1	22.9	16.4	20.3	13.6	14.4
shell	−	1.4	0	5.0	8.3	3.5	6.7
matrix	+	0	9.4	17.8	0	14.7	0
matrix	−	0	0	0	0	0	5.9
Calderwood							
shell	+	5.2	22.1	28.2	21.7	13.3	32.9
shell	−	0	0	5.7	3.6	2.6	6.6
matrix	+	0	0	5.3	0	0	17.7
matrix	−	0	0	0	0	0	5.9
Ardross							
shell	+	0	12.1	6.1	0	0	0
shell	−	0	0	0	0	0	0
matrix	+	0	0	0	0	0	0
matrix	−	0	0	0	0	0	0

acid/asparagine and glutamic acid/glutamine which are present in relatively high levels in the valves of living lingulids (figure 48) as well as the structurally simple aliphatic amino acids, glycine, alanine and valine and the aromatic amino acid tyrosine.

5. CONCLUSIONS

The fossilized shells of *L. squamiformis* from three different horizons of Lower Carboniferous shales and mudstones in Scotland, yield a wealth of information on their original chemico-structure. The evidence includes constituents which have survived more or less in the unaltered state as well as microstructures diagnostic of subtle compositional differences in the stratiform successions of the living shell (figure 51). These data reveal the vertical and areal distribution of the majority of organophosphatic components in the Carboniferous shell which, *in vivo*, must have been indistinguishable from that of Recent *Lingula* in most respects.

(*a*) *Chemico-structural homologies of Carboniferous and Recent shells*

The living *L. squamiformis* shell was flexible, a property which survived death and at least the early stages of diagenesis and rock formation. This retention of plasticity is revealed by the tendency of the valves to wrinkle into impersistent transverse folds and to become moulded around clastic grains (up to 150 μm in size) without fracturing, in response to uneven loading during compaction of the entombing sediments (figures 4 and 11). The principal components of the shell, imparting this flexibility, would have been GAGs; and there are good indicators of their precise distribution throughout the living integument.

The fossilized primary layer which is composed of variably kaolinized spherular apatite bears superficial traces of drape sets, clusters of hemispherical hollows and parallel grooves (figures 8–10). The interpretation of these microstructures as strain figures and as moulds of vesicular cell features respectively, implies that the primary layer was secreted as a plastic medium. The primary layer of living *L. anatina* has been shown by Alcian Blue staining to consist almost exclusively of acidic GAGs (Williams *et al.* 1994, p. 248). It is, therefore, assumed that GAGs were prevalent in the *L. squamiformis* primary layer and were replaced by kaolinite during later stages in shell fossilization.

GAGs are also an important constituent of the secondary layer of living *L. anatina*, where they fill all spaces in the biomineral framework of virgose laminae and occur in sufficient quantities to impose a vertical cleavage on compact laminae. The occurrence of cleavage and spaces (partly filled by kaolinite and recrystallized apatite with clay traces) in the *L. squamiformis* secondary shell (figures 7, 17 and 34), confirms the prevalence of GAGs in this layer in the living state.

It is noteworthy that even the clay fraction of the shell itself is consistent with its formation in an acidic GAGs. In all three samples, but especially well shown in some Calderwood specimens, books of kaolinite within *L. squamiformis* shells contrast with the blades and laths of potassium-bearing illite of the sedimentary matrix (Williams & Cusack 1995). The biomineral constituents of living *L. squamiformis* must have been indistinguishable from those of Recent *L. anatina* in their mode of aggregation and their stratiform accretion. The distribution of apatite in fossilized *L. squamiformis* shells, however, is different in two respects.

First, the preserved primary layer contains a much higher proportion of spherular apatite. This could have resulted from recrystallization which, elsewhere in the shell, is manifest in cavities within virgose laminae and along microfractures, laminar interfaces and the bounding surfaces of valves. Yet the marginal folds of the *L. squamiformis* valves, which would have consisted of the outer part of the primary layer and the overlying periostracum, appear not to have been preserved. Such selective recrystallization is much less likely to have occurred than the secretion of significant amounts of authigenic spherular apatite as well as GAGs during deposition of the inner part of the primary layer as occurs in living *Discina* (Williams *et al.* 1992, p. 86).

Secondly, a much higher proportion of authigenic apatite is also characteristic of the anteriomedian sectors of the secondary layers of the *L. squamiformis* shell. In contrast, the anteriomedian sectors of the secondary layers of the *L. anatina* shell contain negligible amounts of disorientated spherular apatite in laminae mainly composed of GAGs. This difference explains the contrast between the smoothly rounded anterior margins (figure 5) of disarticulated *L. squamiformis* valves from Calderwood and the fretted margins of bleached Recent *L. anatina* valves (figure 1) accumulating under comparable conditions of exposure to degrading fluids.

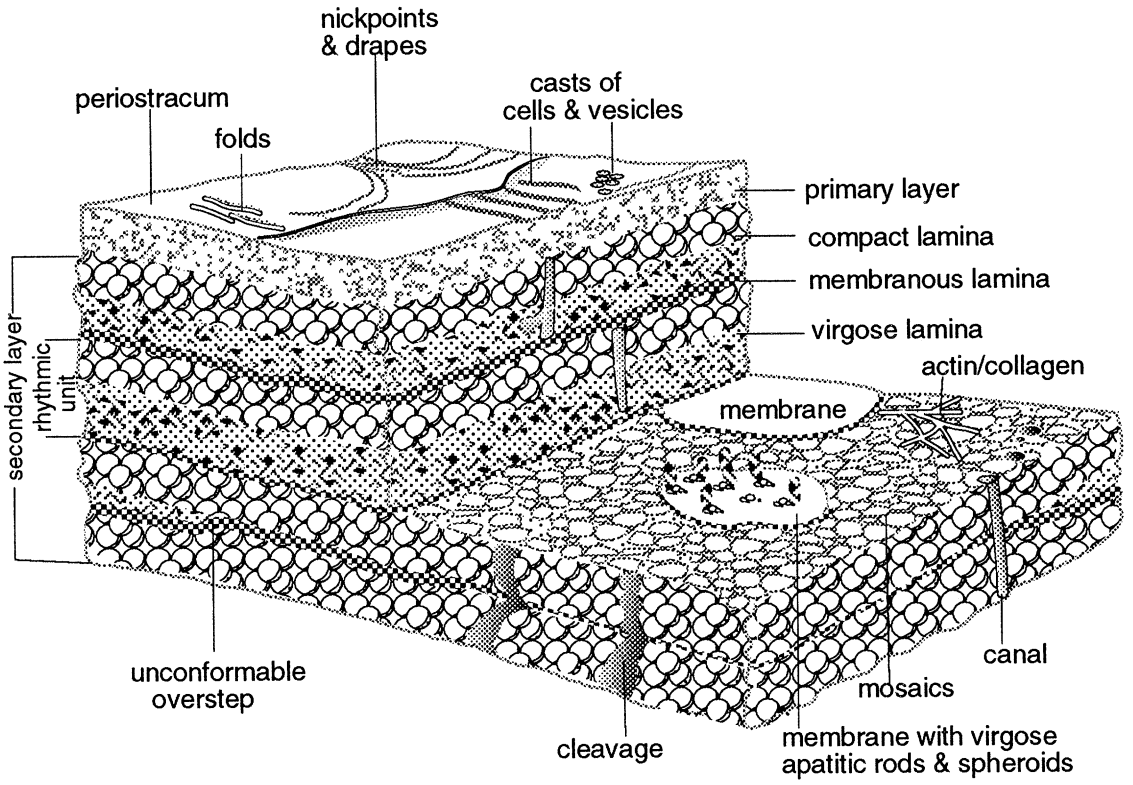

Figure 51. Diagrammatic reconstruction of the laminar succession in the mid-region of a mature, living valve of *Lingula squamiformis* from the Lower Carboniferous of Scotland.

The presence of degraded residues of some organic constituents (other than GAGs) of the living *L. squamiformis* shell, has been confirmed structurally as well as biochemically. The occurrence of apatite mainly in spherular form suggests that the chitino-proteinaceous coats of these aggregates persisted until after the degradation of the GAGs matrix as presumably did chitinous fibrils imparting the horizontal lineation on the biomineral components of compact laminae.

There is also direct evidence of another organic constituent, rarely exposed as discrete strands in rod laminae or as a web on the interior of a Kinghorn valve (figures 37 and 41). These strands, which are currently known only as scanning electron microscope (SEM) images, compare in habit and thickness with collagenous mats in the *L. anatina* shell (Williams *et al.* 1994). They are, however, also similar to webs seen beneath the periostracum in a critical point dried *L. anatina* and at the interface between membranous and compact laminae of *G. pyramidata* (figures 44–47). These latter webs have been provisionally identified as part of the terminal actin cortex of secreting outer epithelium, which is periodically incorporated within the shell after the sloughing off, and digestion, of the covering plasmalemma. Muscle actin contains 375 amino acids (Vandekerckhove & Weber 1979) and has a molecular mass around 40 kDa. The 36 kDa protein (as estimated by polyacrylamide gel electrophoresis) extracted from *L. anatina* valves (Williams *et al.* 1994) will be examined more closely.

The much higher concentration of amino acids in the posterior parts of valves of *L. anatina* and *G. pyramidata* relative to the anterior parts is consistent with the observation (Williams *et al.* 1994) that apatitic spheroids with proteinaceous coats are the main constituent of the posteriomedian body platform, whereas the highly organic anteriomedian sector of a valve is composed mainly of GAGs. Moreover, the high level of hydroxyproline in the posterior parts of *L. anatina* and *G. pyramidata* valves is consistent with the discovery that mats of fibrillar collagen occur in the body platform of *L. anatina* (Williams *et al.* 1994).

Of the Carboniferous samples, those from Kinghorn and Calderwood contain the acidic amino acids or their amine form, aspartic acid/asparagine and glutamic acid/glutamine, which are present in relatively high levels in the valves of living lingulids (figure 48) and are generally associated with phosphatic and carbonate biomineralized structures. In addition, the structurally simple, aliphatic amino acids, glycine, alanine and valine, which may partly result from degradation of more complex amino acids, are present in the Kinghorn and Calderwood valves as well as the aromatic amino acid tyrosine. The Ardross samples are heavily pyritized as a result of sulphate reduction and a concomitant extensive degradation of organic material is indicated by the low level and range of amino acids present i.e. glutamic acid/glutamine and glycine (table 1).

In respect of its stratiform succession as a whole, *L. squamiformis* is again indistinguishable from *L. anatina*. The laminar sequence of Carboniferous lingulas (figures 7 and 17) conform to the same rhythmic sets and are permeated by an identical system of canals, chambers and galleries as characterize their living

descendants. Only the average thickness of the fully developed laminar cycle is different and that could well have been phenotypically controlled.

(*b*) *Implications of the degradation of Carboniferous Lingula shells*

Notwithstanding such intricate chemico-structural homologues of the shells of Carboniferous and Recent *Lingula*, compositional differences confound the assumption that only catastrophic events (sudden changes in salinity, temperature, rates of sedimentation and stability of the substrate) can lead to fossilization of lingulid shells (Emig 1990, p. 234). Emig's conclusions on *post mortem* chemical degradation and mechanical abrasion of lingulid shells were based on studies of subtidal populations of *L. anatina* in Japan and New Caledonia and *L. reevii* in Hawaii. He found that the margins of dead shells were rapidly degraded and thereafter the biomineralized laminae abraded so quickly that even the thickest part, the body platform, was normally reduced to 'unrecognizable fragments' within three weeks (Emig 1990, p. 234). The chemical degradation of the shell can be simulated by bleaching valves (figure 1); which confirms Emig's observations on the rapid disintegration of their margins.

This disintegration of Recent lingulid shells is greatly facilitated when valves are disarticulated. Morse (1902, p. 318) noted that the death of *Lingula* through natural causes is signalled by the emergence of the shell from the burrow which, however. continues to accommodate the pedicle. The shell, lying on the seabed, then decomposes and may subsequently float away from the buried pedicle even in a gentle agitation of water.

The size-frequency distributions of flat-lying shells and valves from the shales at Calderwood and Kinghorn suggest that these assemblages accumulated near their burrows as residual fossil communities. They would certainly have been exposed to chemico-physical weathering for at least as long as any dead *Lingula* accumulating today. Yet these Carboniferous residues are largely composed of valves, some no longer than 2 mm and no thicker than 20 μm, which are complete except for marginal folds. The fossilization of such complete valves confirms that the shell of living *L. squamiformis* had a higher and more uniformly distributed apatitic content than that of Recent species.

In respect of stock survival, this difference in composition could have affected the relative flexibility of the anteriomedian sectors of the shell. In living *Lingula*, the sectors are mainly composed of GAGs and bend outwards to form a biconvex funnel containing the three setal pseudosiphons, by which seawater is circulated within the mantle cavity. The anteriomedian sectors of *L. squamiformis* with their comparatively high apatitic content could have been more brittle and accordingly less favoured by natural selection during the evolution of the *Lingula* shell (Williams *et al.* 1994, p. 261). On the other hand, the apatite in the anteriomedian sectors would have been distributed as organically coated spherules and, in life, would have acted like ball-bearings in a gel. In effect, the relative merits of flexibility and strength were probably finely balanced during the evolution of this part of the lingulid shell.

We thank Dr Neil Clark of the Hunterian Museum, who led the collecting visit to Ardross, provided photographs of *L. squamiformis* and placed his expertise on the Scottish Carboniferous at our disposal. We also thank Professor Gordon Y. Craig of Edinburgh University, who introduced us to the Kinghorn succession, Dr Gordon B. Curry of Glasgow University, who gave us the Calderwood material, Mr. Peter Aynsworth, Mr Douglas McLean and Ms Sandra McCormack of the Department of Geology and Applied Geology in Glasgow University for their technical and photographic assistance, and Dr. Mark Dean of the British Geological Survey and Dr Ian Rolfe of the National Museums of Scotland who loaned us specimens. The work was funded by NERC (grant number GR3/09604) and The Royal Society (grant number RSRA/C.027) to M.C.

REFERENCES

Biernat, G. & Emig, C. C. 1993 Anatomical distinctions of the Mesozoic lingulide brachiopods. *Acta Palaeont. Polon.* **38**, 1–20.

Cater, J. M. L., Briggs, D. E. G. & Clarkson, E. N. K. 1989 Shrimp-bearing sedimentary successions in the Lower Carboniferous (Dinantian) Cementstone and Oil Shale Groups of northern Britain. *Trans. R. Soc. Edinb.* **80**, 5–15.

Clark, N. D. L. 1989 Carboniferous coprolitic bacteria from the Ardross Shrimp Bed, Fife. *Scott. J. Geol.* **25**, 99–104.

Craig, G. Y. 1952 A comparative study of the ecology and palaeoecology of *Lingula*. *Trans. Edinb. geol. Soc.* **15**, 110–120.

Emig, C. C. 1981 Implications de données récentes sur les Lingules actuelles dans les interprétations paléoécologiques. *Lethaia*, **14**, 151–156.

Emig, C. C. 1984 Importance de sediment dans la distribution des Lingules. *Lethaia*, **17**, 115–123.

Emig, C. C. 1986 Conditions de fossilisation du genre *Lingula* (Brachiopoda) et implications paléoécologiques. *Palaeogeogr. Palaeoclimatol., Palaeoecol.* **53**, 245–253.

Emig, C. C. 1990 Examples of post-mortality alteration in Recent brachiopod shells and (paleo)ecological consequences. *Mar. Biol.* **104**, 233–238.

Ferguson, L. 1962 The paleoecology of a Lower Carboniferous marine transgression. *J. Paleont.* **36**, 1090–1107.

Ferguson, L. 1963 The paleoecology of a *Lingula squamiformis* Phillips during a Scottish Mississippian marine transgression. *J. Paleont.* **37**, 669–681.

Graham, D. K. 1970 Scottish Carboniferous Lingulacea. *Bull. geol. Surv. Gr. Br.* **31**, 139–184.

Jin, Y.-G, Wang, H.-Y & Wang, W. 1991 Palaeoecological aspects of brachiopods from Chiungchussu Formation of early Cambrian age, Eastern Yunnan, China. In *Palaeoecology of China* (ed. Y.-G. Jin, J.-G. Wang & S.-H. Xu), pp. 25–47. Nanjing University Press.

Morse, E. S. 1902 Observations on living Brachiopoda. *Boston Soc. Nat. Hist., Memoir* **5**, 313–386.

Paine, R. T. 1970 The sediment occupied by recent lingulid brachiopods and some palaeoecological implications. *Palaeogeogr., Palaeoclimatol., Palaeoecol.* **7**, 21–31.

Plaziat, J.-C., Pajaud, D., Emig, C. & Gall, J.-C. 1978 Environnements et distribution bathymétrique des Lingules actuelles; conséquences pour les interprétations paléogéographiques. *Bull. Soc. géol. Fr.* **7**, 309–314.

Vandekerckhove, J. & Weber, K. 1979 The complete amino acid sequence of actins from bovine aorta, bovine

heart, bovine fast skeletal muscle, and rabbit slow skeletal muscle. *Differentiation* **14**, 123–133.

Williams, A., Mackay, S. & Cusack, M. 1992 Structure of the organo-phosphatic shell of the brachiopod *Discina*. *Phil. Trans. R. Soc. Lond.* B **337**, 83–104.

Williams, A., Cusack, M. & Mackay, S. 1994 Collagenous chitinophosphatic shell of the brachiopod *Lingula*. *Phil. Trans. R. Soc. Lond.* B **346**, 223–266.

Williams, A. & Cusack, M. 1995 Brachiopod (lingulid) shell mediation in clay formation. (In the press.)

Received 30 June 1995; accepted 2 August 1995

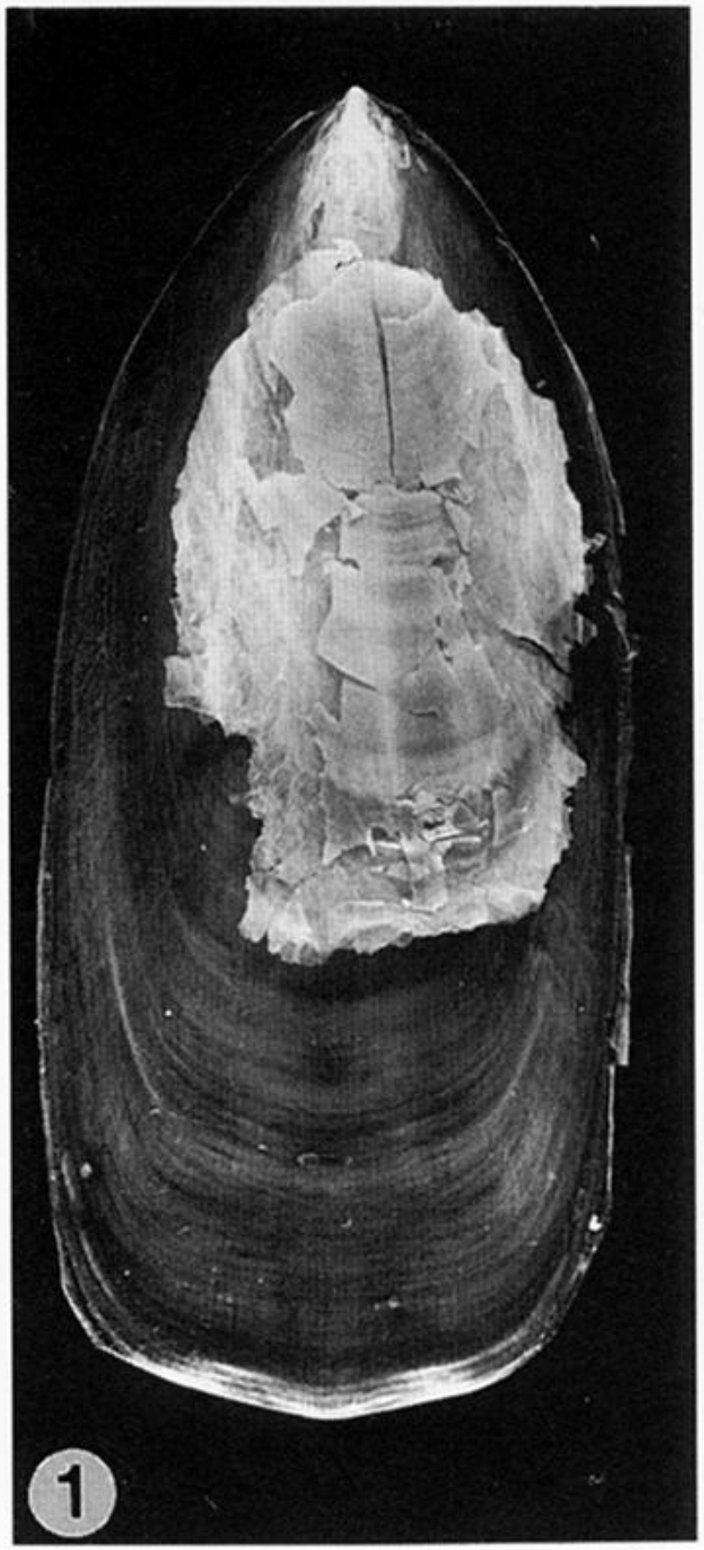

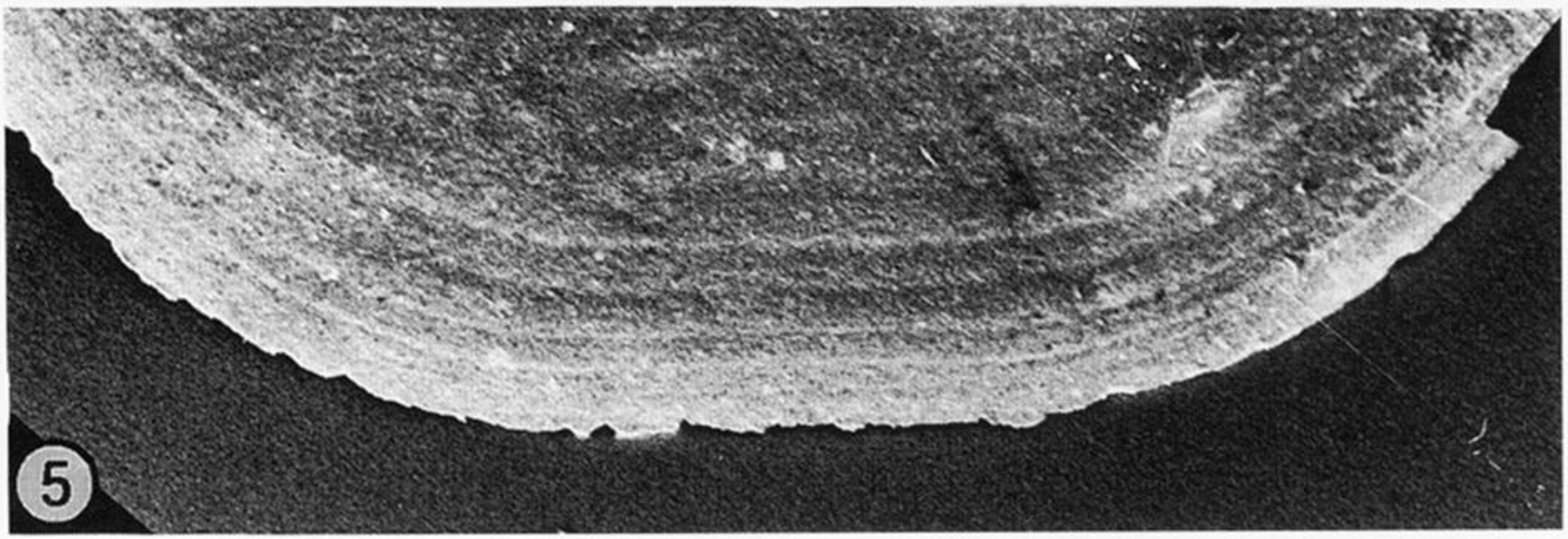

Figure 1. External view of the ventral valve of *Lingula anatina* in the background with the remains (treated with 40% sodium hypochlorite for 24 h) of the matching dorsal valve superimposed. ×2.4 natural size.

Figure 2. Skewed valves of a complete shell of *Lingula squamiformis* from Kinghorn. ×2.1 natural size.

Figures 3 and 4. External views of dorsal valves of *Lingula squamiformis* from Calderwood showing general shape and the wrinkling of shell. ×5 and ×6 natural size, respectively.

Figure 5. SEM of the anteriomedian margin of the valve of *Lingula squamiformis* from Calderwood showing the complete phosphatization of the anterior margin. ×35 natural size.

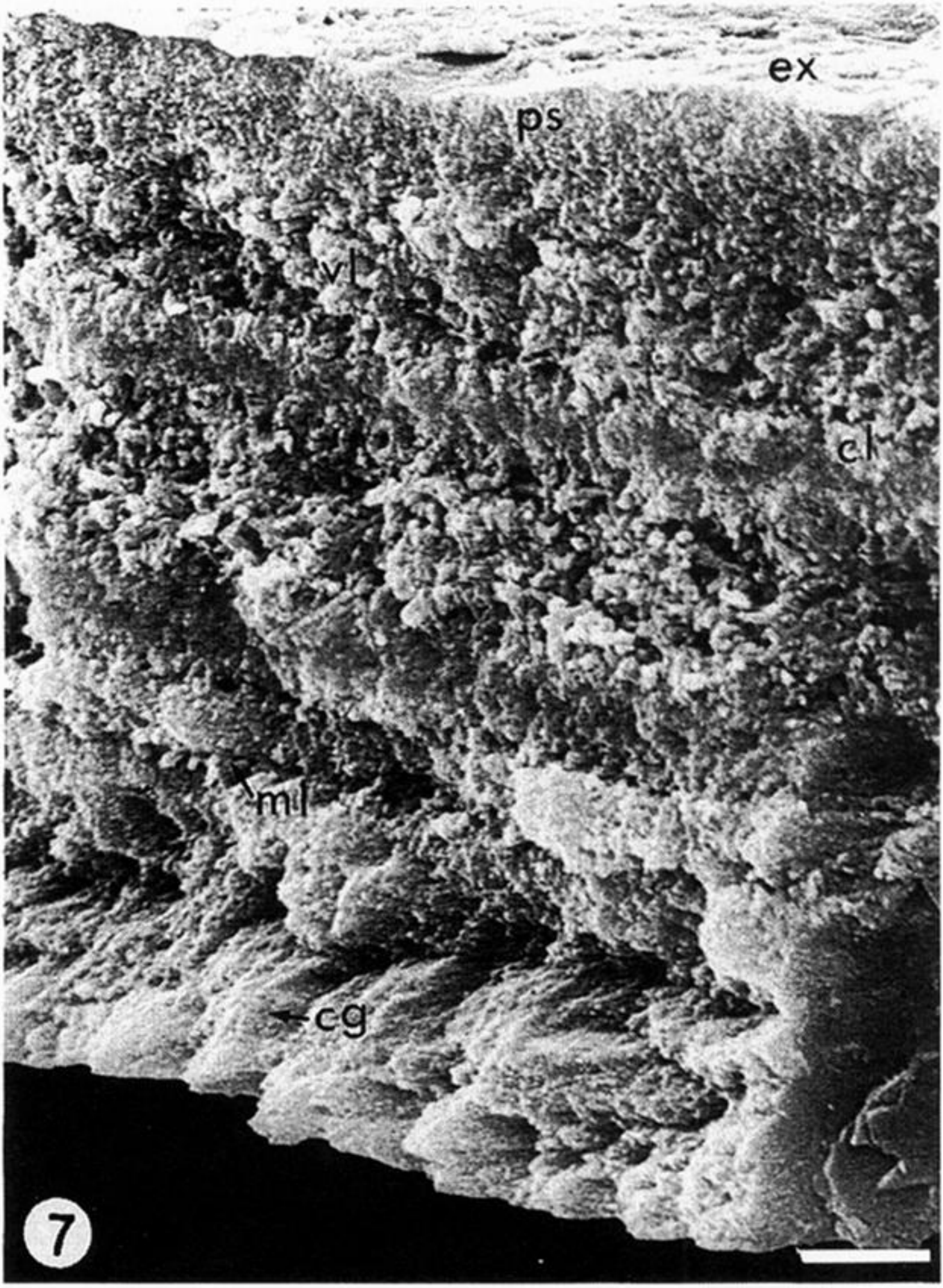

Figure 7. SEM of a gold-coated vertical fracture section of a valve of *L. squamiformis* from Calderwood showing the general succession of primary shell (ps) at the external surface (ex) underlain by sets of membranous (ml), compact (cl) and virgose (vl) laminae, affected by vertical cleavage (cg). Scale bar = 2 μm.

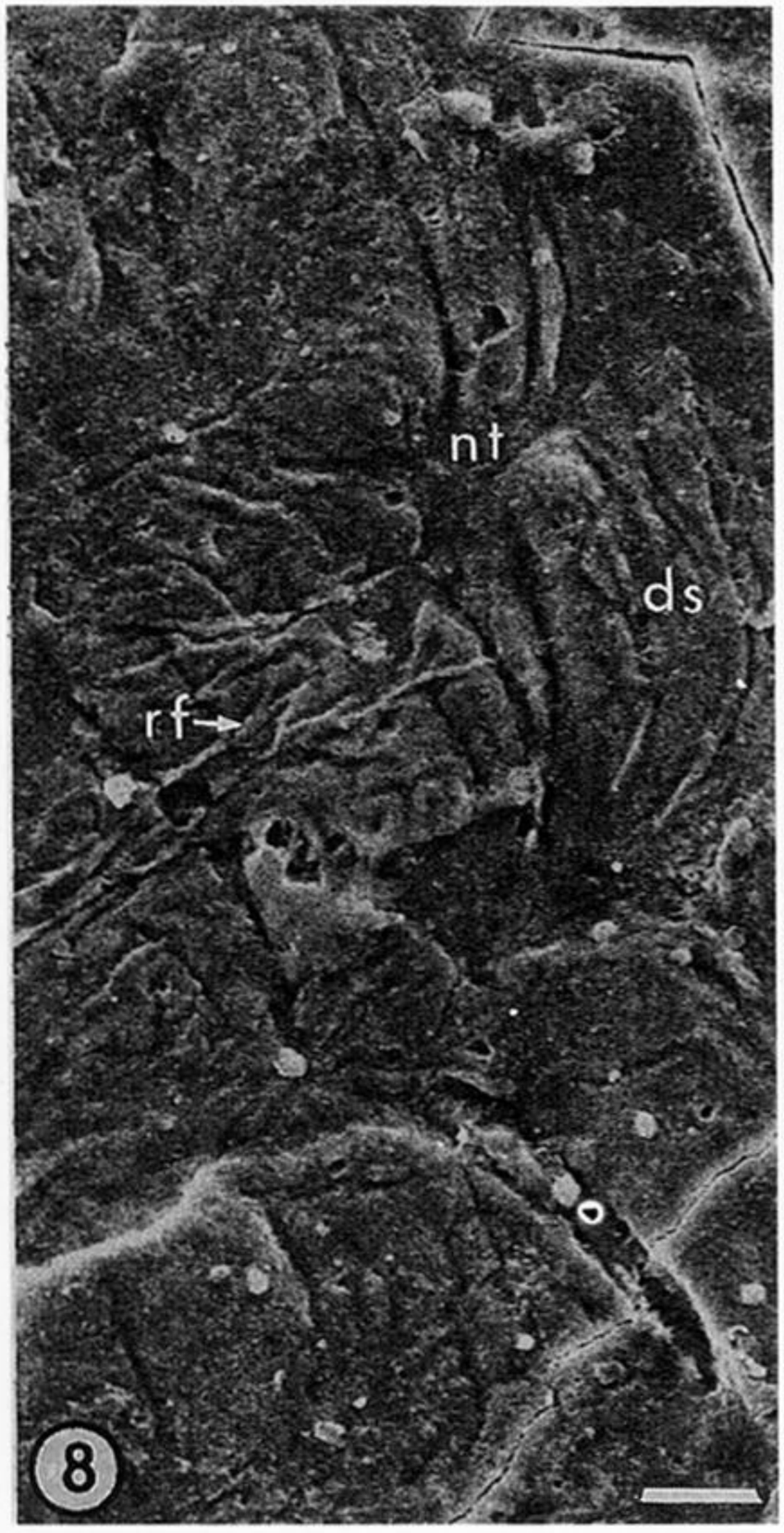

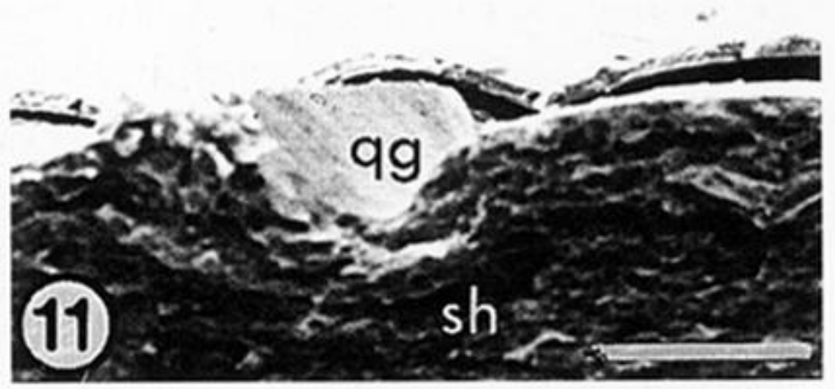

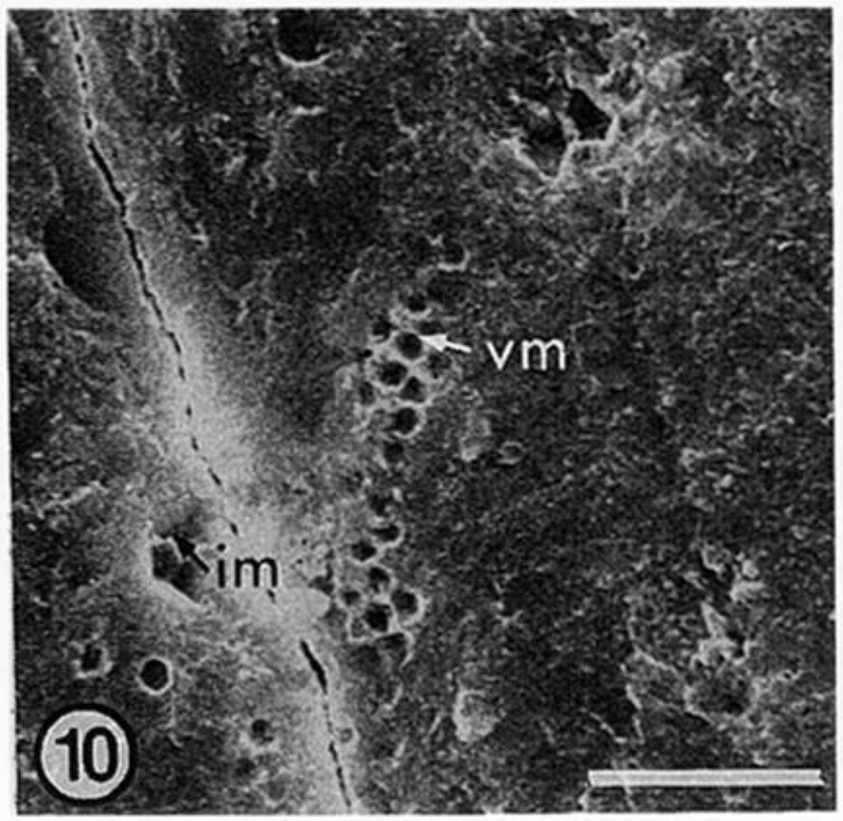

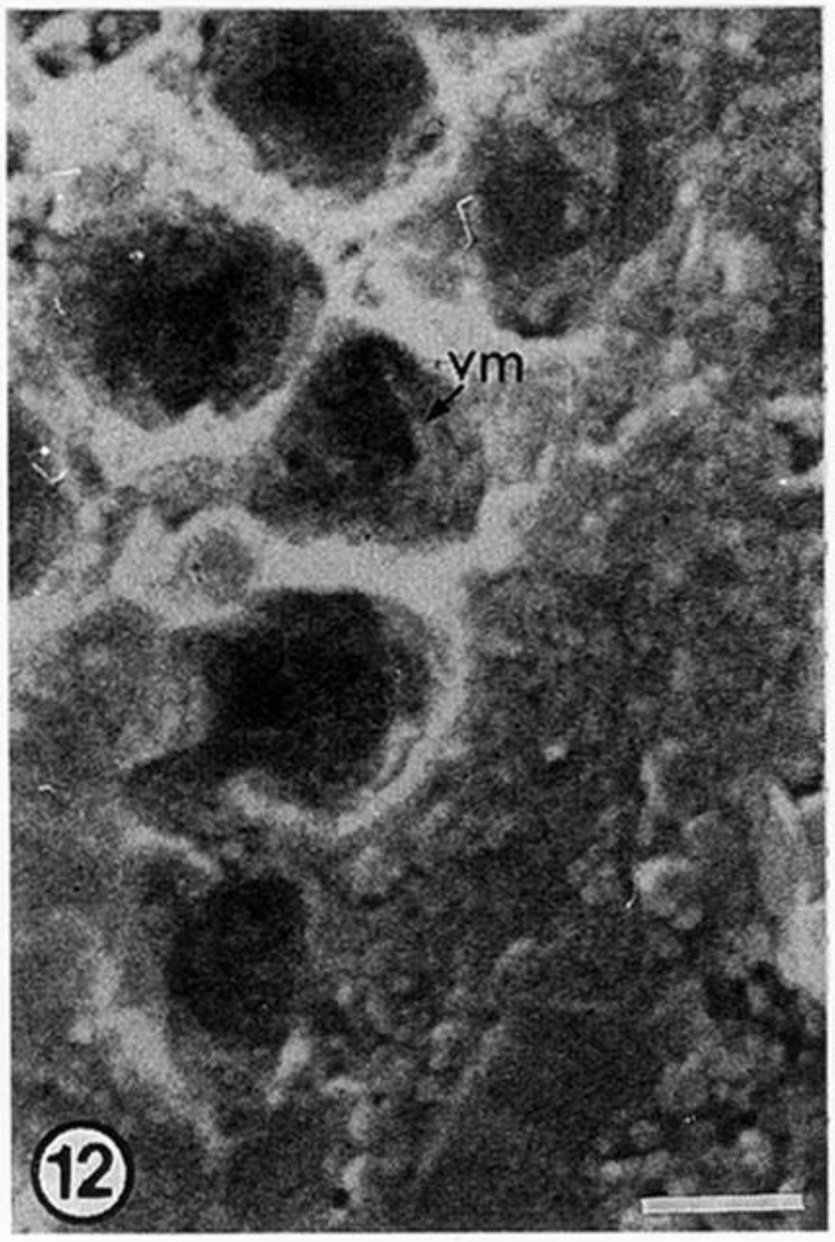

Figures 8–12. SEMs of gold-coated external surfaces and one fracture section of valves of *L. squamiformis* from Calderwood.

Figure 8. Surface deformed by drapes (ds) and nickpoints (nt), and radial folds (rf). Scale bar = 10 μm.

Figure 9. Moulds (ib) of thickened intercellular deposits defining vesicular cells orthogonal to a growth edge (gr). Scale bar = 25 μm.

Figures 10 and 12. General view and detail of moulds (vm) of a close packed raft of vesicles, with impact moulds (im) of coarser clastic grains in entombing sediment. Scale bars = 5 μm and 500 nm, respectively.

Figure 11. Fracture section showing a valve as a thin sinuous band bending around a quartz grain (qg) in the shale (sh). Scale bar = 100 μm .

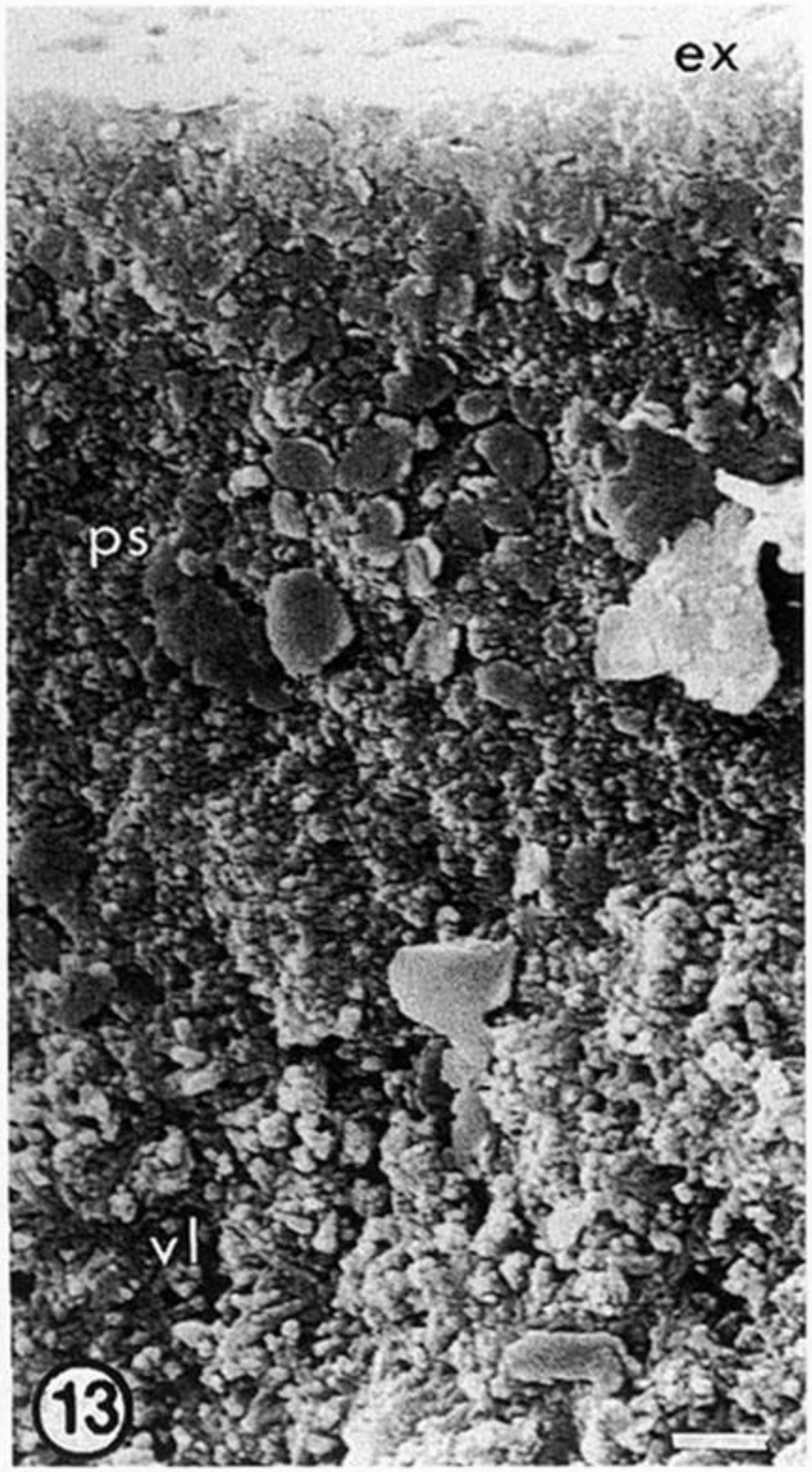

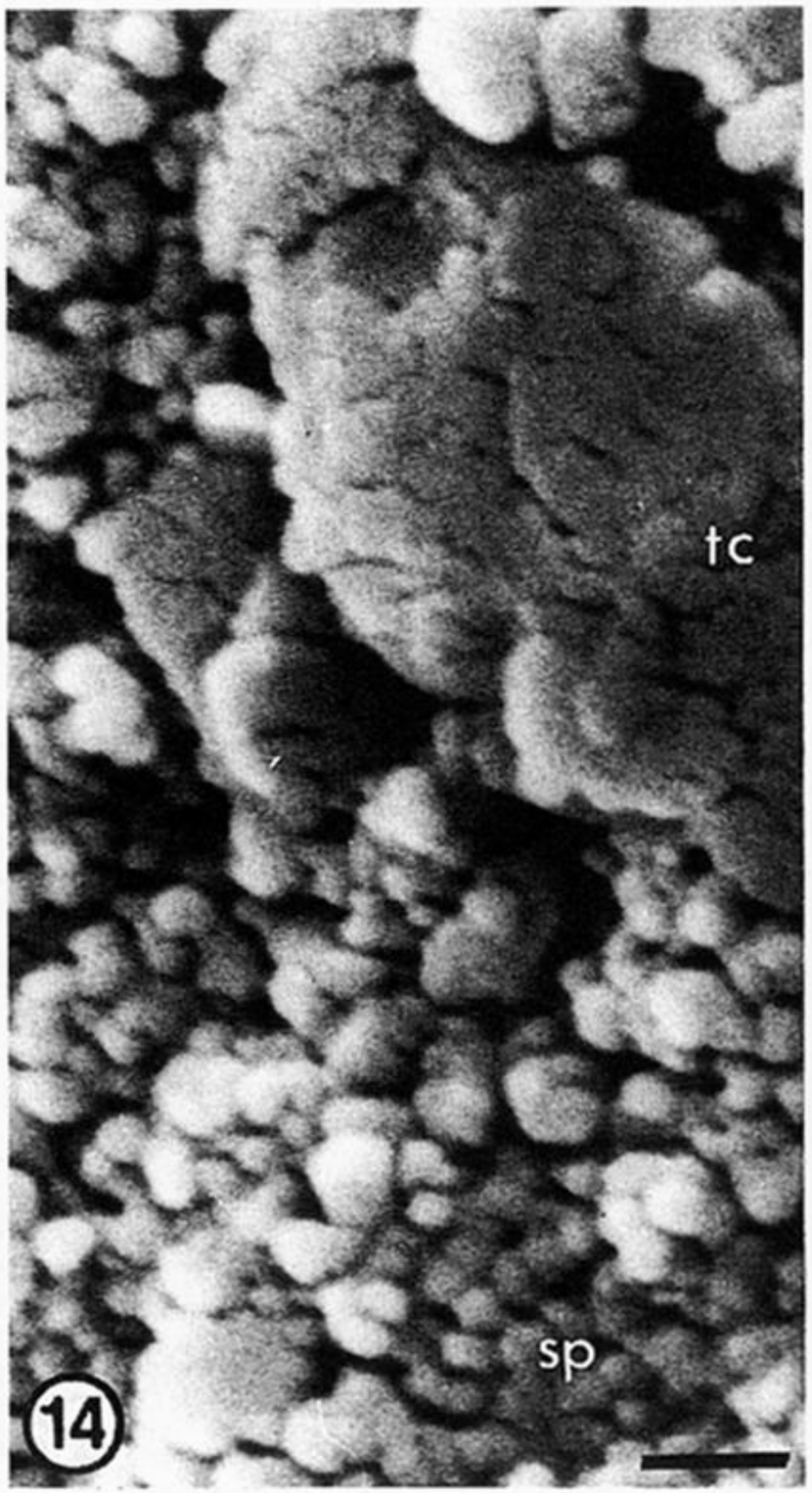

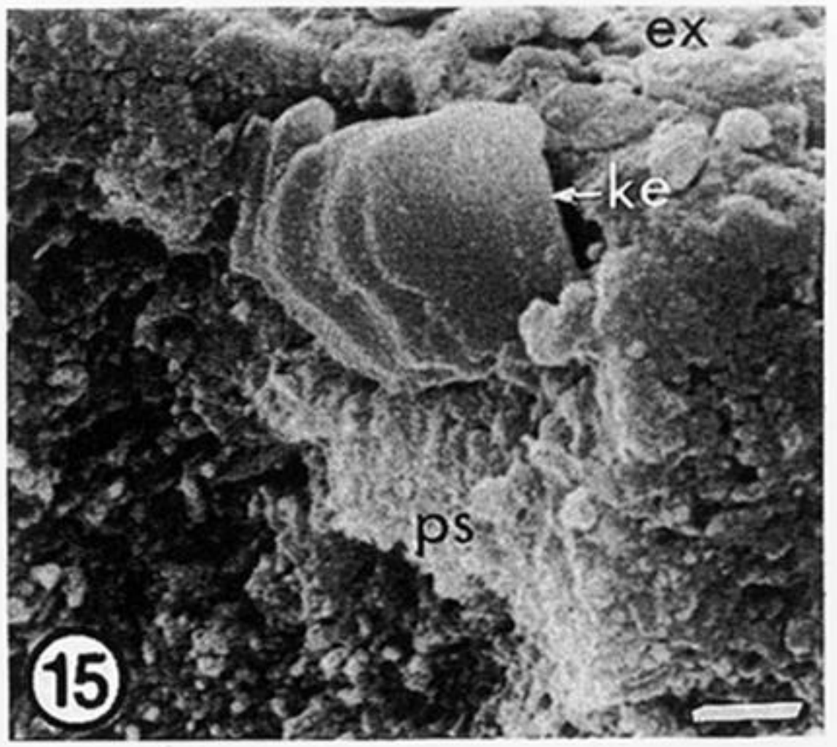

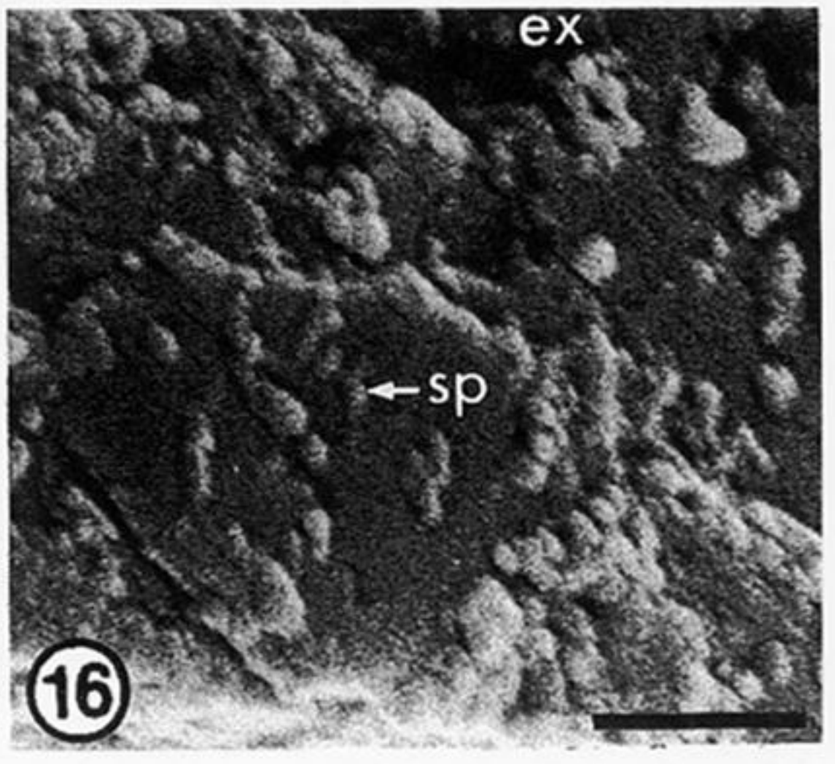

Figures 13–16. SEMs of gold-coated vertical fracture sections of valves of *L. squamiformis* from Calderwood.

Figures 13 and 14. General view and detail of primary layer (ps), forming the external surface (ex) and succeeded by a virgose lamina (vl), with dehydrated recrystallized patches of tension-cracked (tc) apatite with clay and spherular apatite (sp) surviving more or less intact. Scale bars = 1 μm and 250 nm, respectively.

Figure 15. Primary layer (ps) immediately below the external surface (ex) of a valve containing a book of kaolinite (ke). Scale bar = 1 μm.

Figure 16. Primary layer immediately below the external surface consisting of recrystallized pinacoids of apatite with kaolinite traces, partly incorporating apatitic spherules (sp). Scale bar = 1 μm.

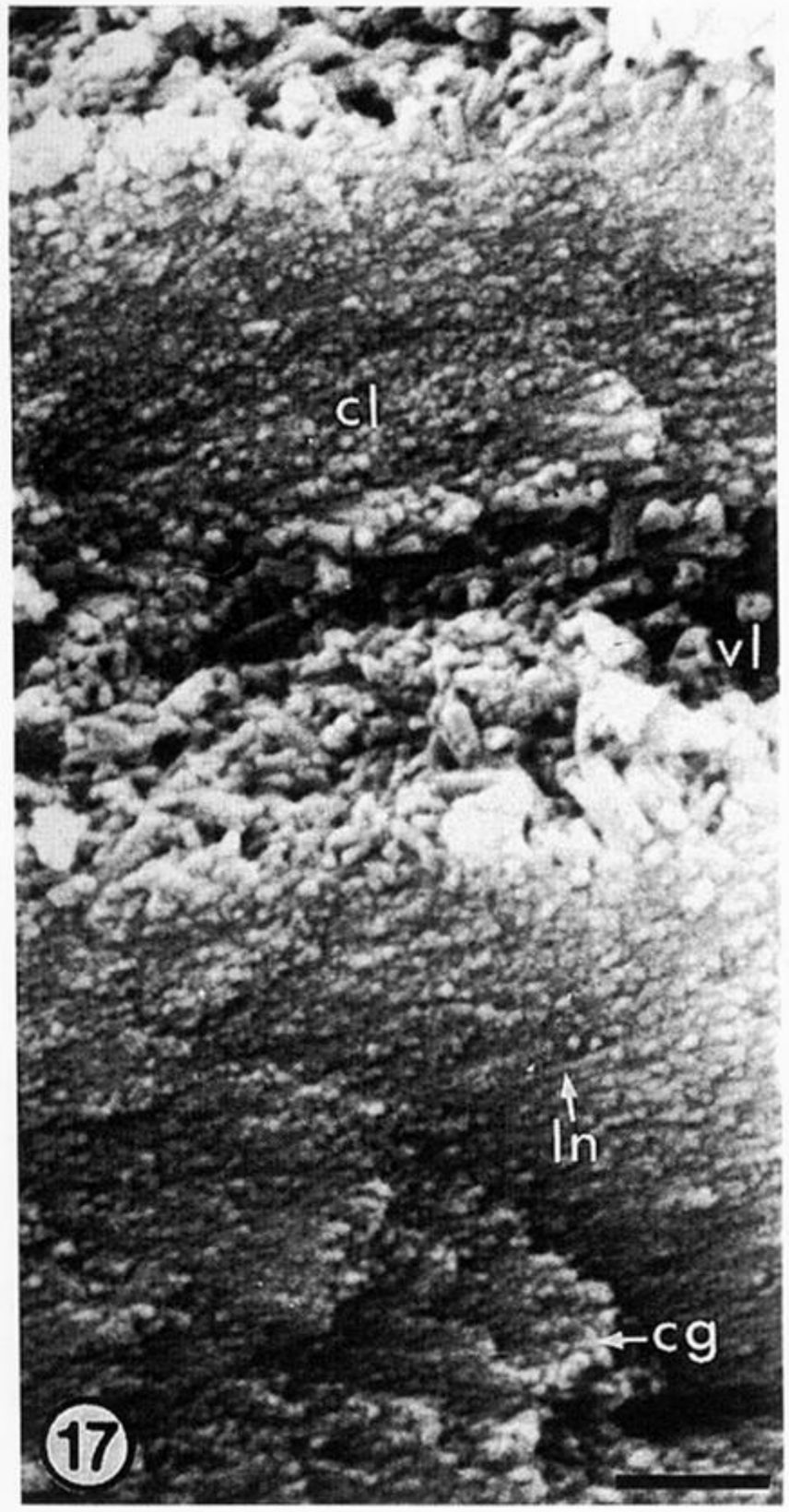

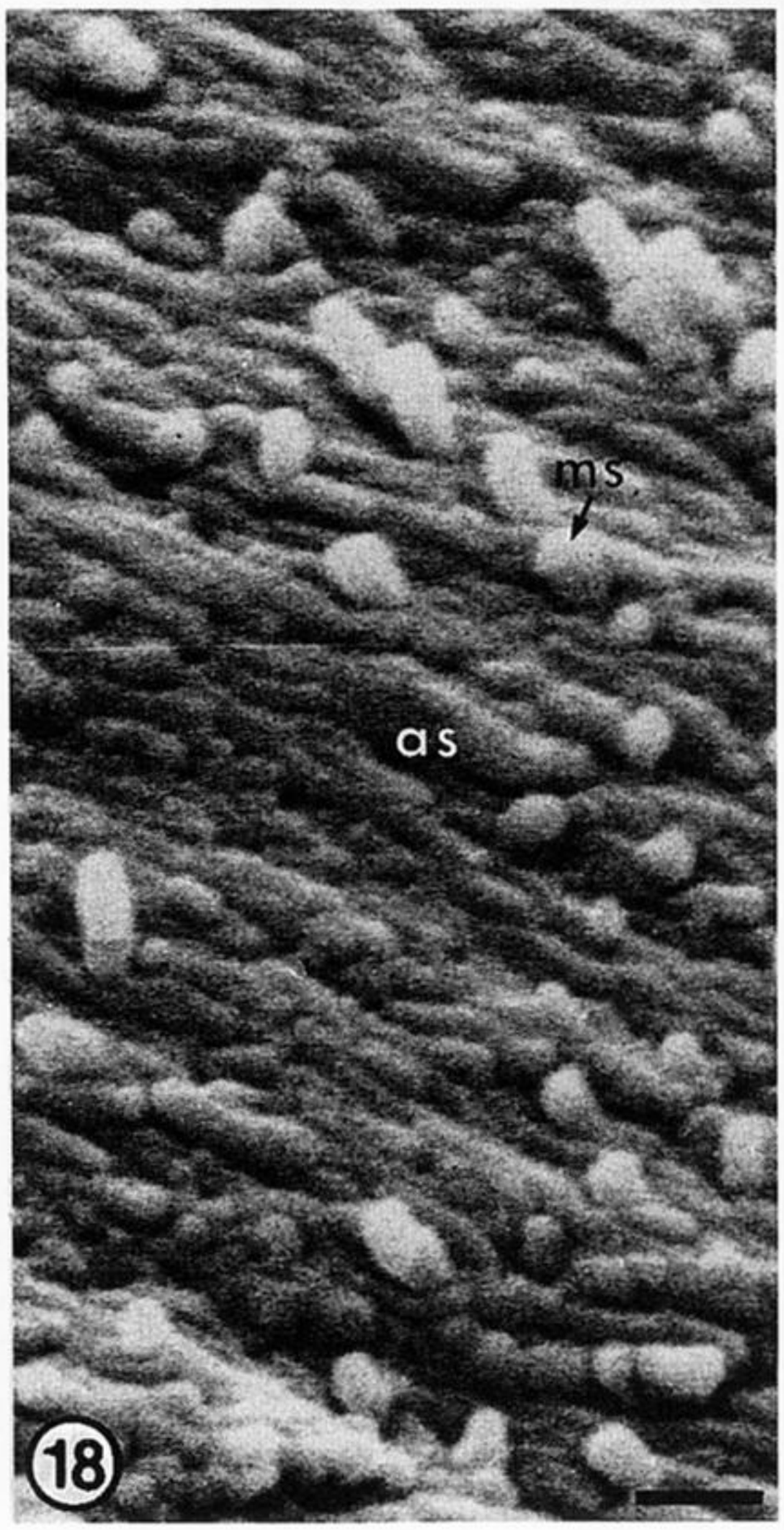

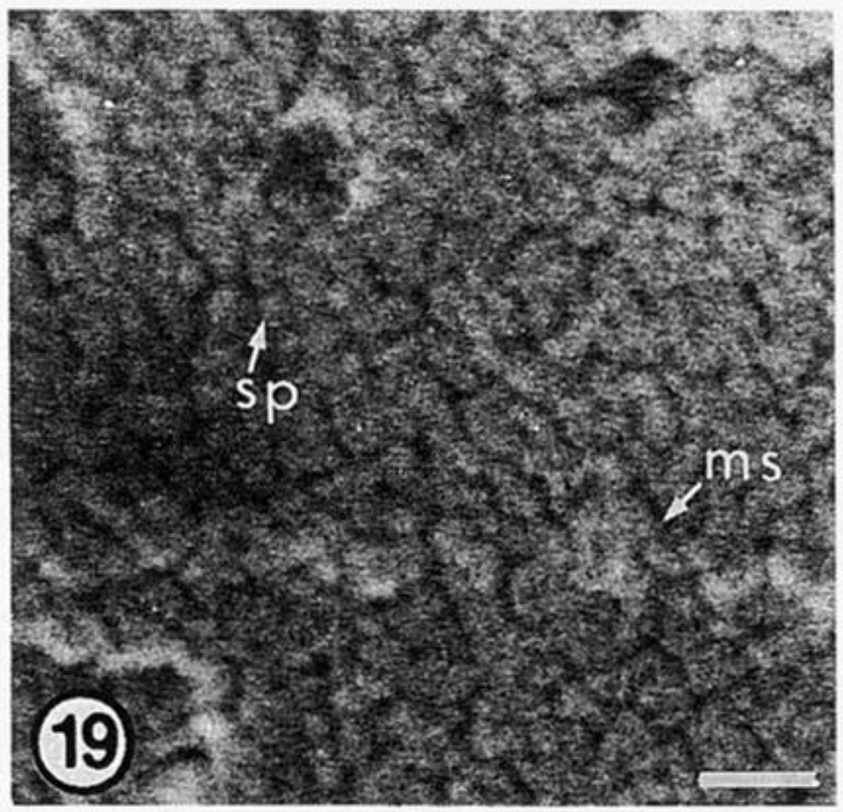

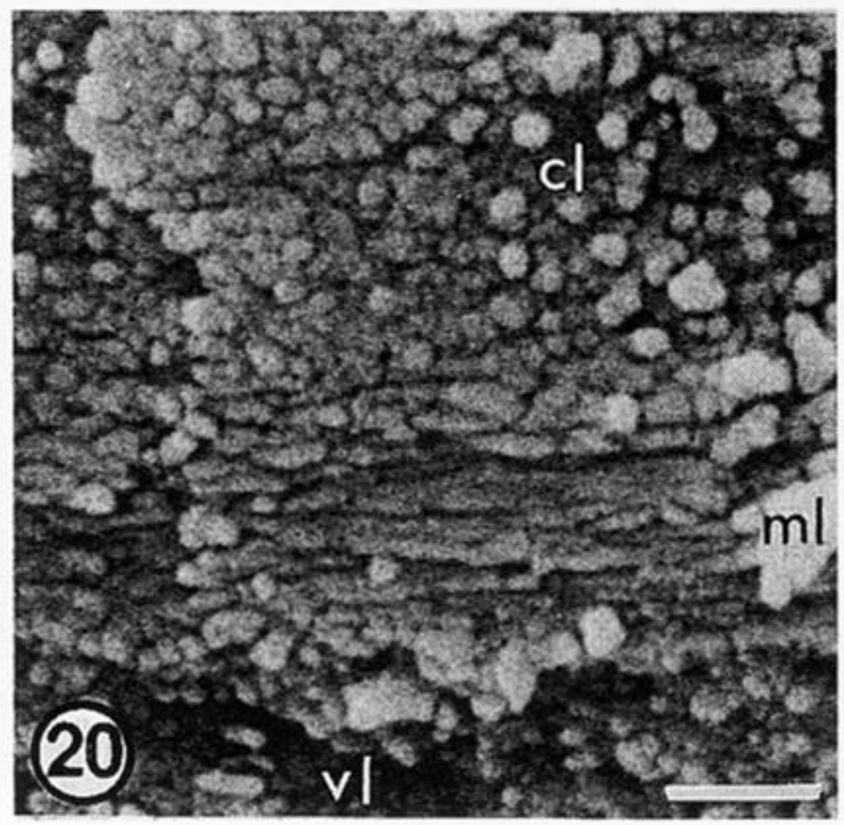

Figures 17–20. SEMs of gold-coated vertical fracture sections and an internal surface (figure 19) of valves of *L. squamiformis* from Calderwood.

Figure 17. Compact laminae (cl), interleaved with virgose laminae (vl), showing lineation (ln) and cleavage (cg). Scale bar = 1 μm.

Figure 18. Detail of a lineated compact lamina composed of 'worm-like' arrays of spherules (as) and larger mosaics (ms). Scale bar = 250 nm.

Figure 19. External surface view of a compact lamina showing the range of granular aggregates from spherules (sp) to mosaics (ms). Scale bar = 250 nm.

Figure 20. Recrystallized membranous lamina (ml) intercalated between the base of a compact lamina (cl) and the top of a virgose lamina (vl). Scale bar = 500 nm.

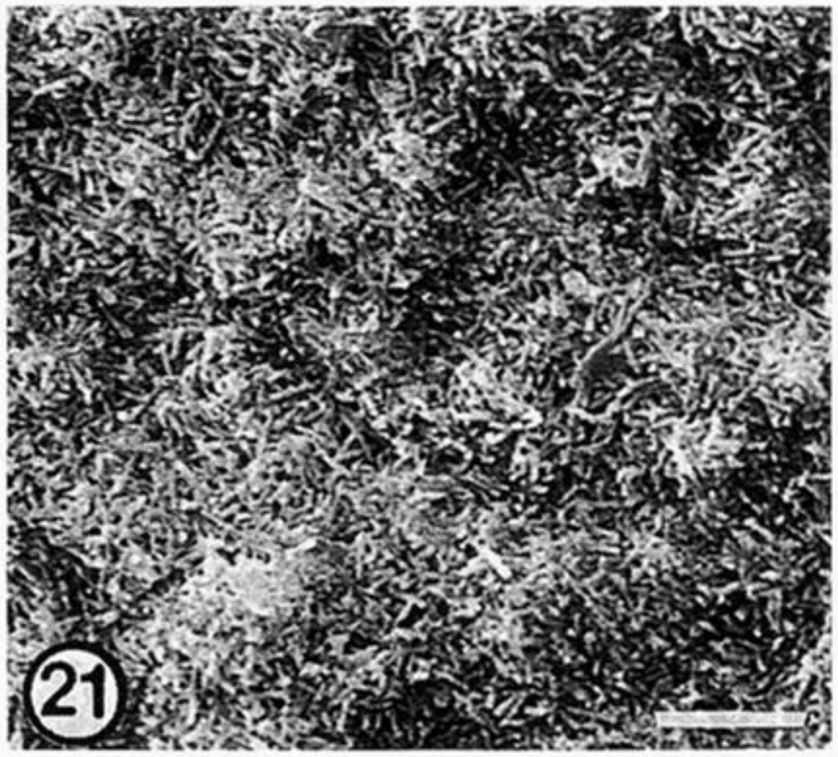

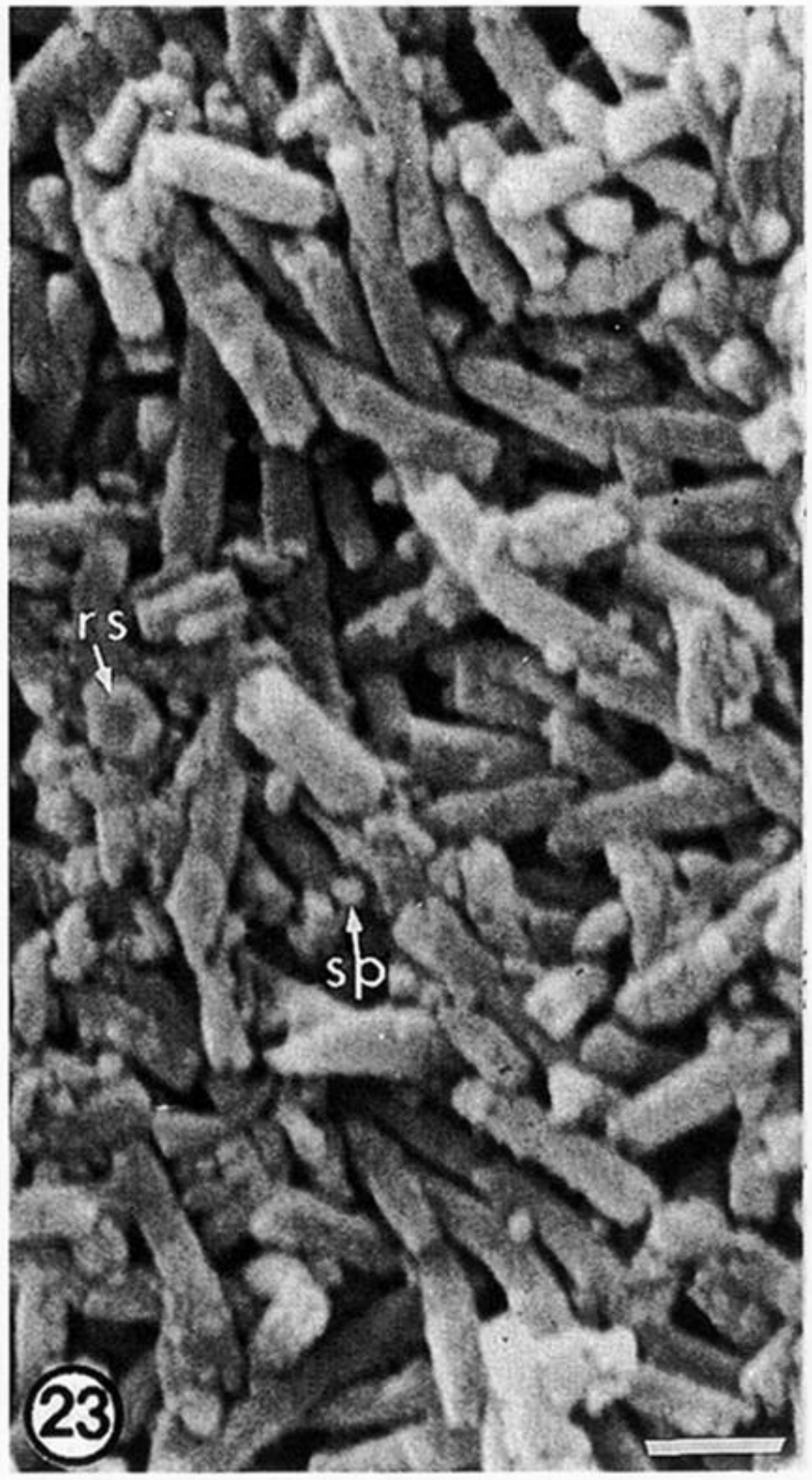

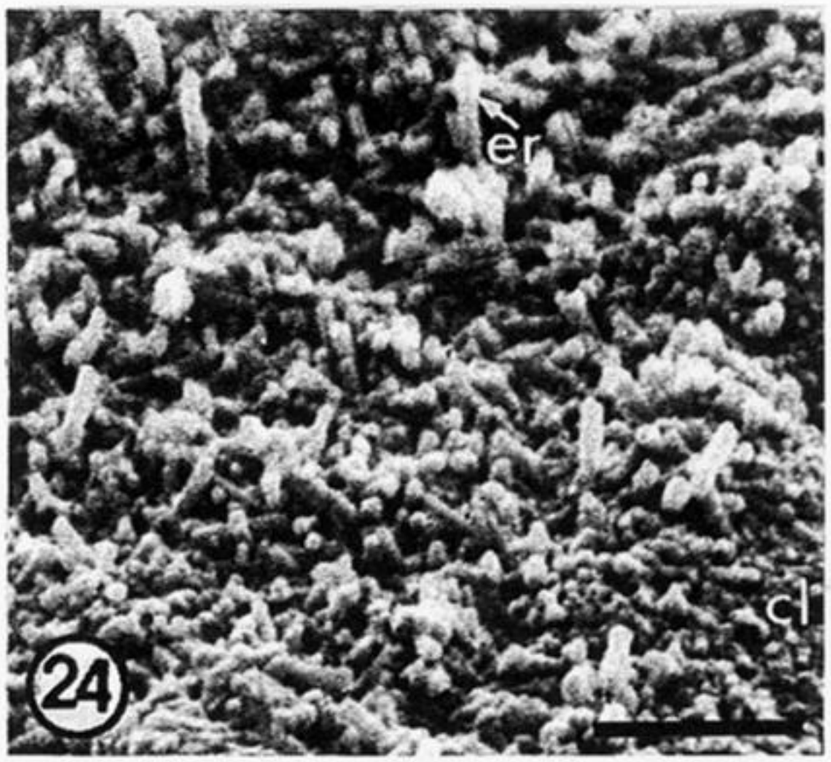

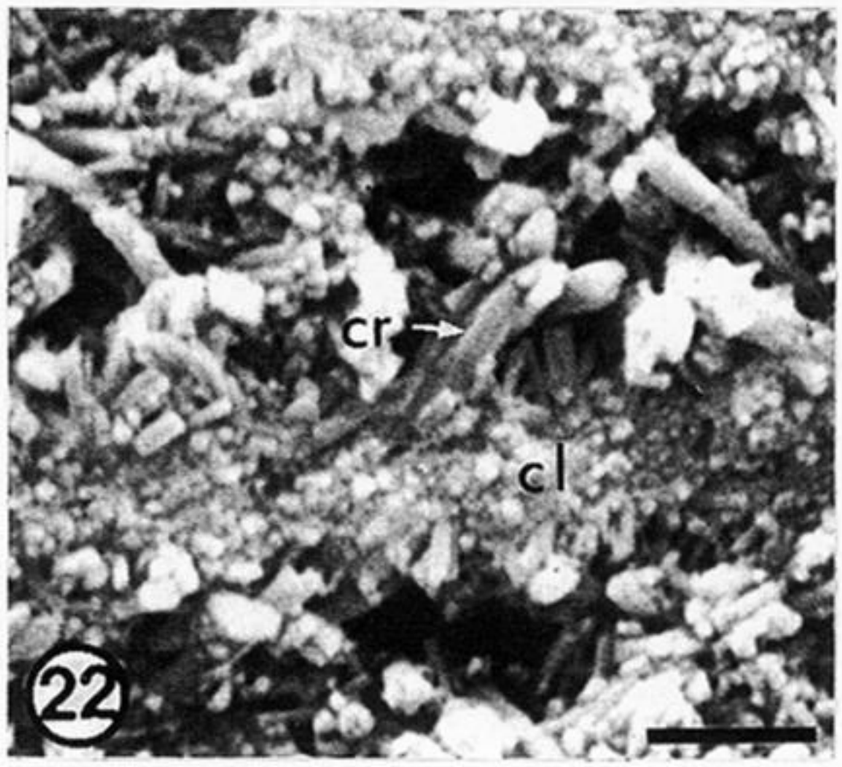

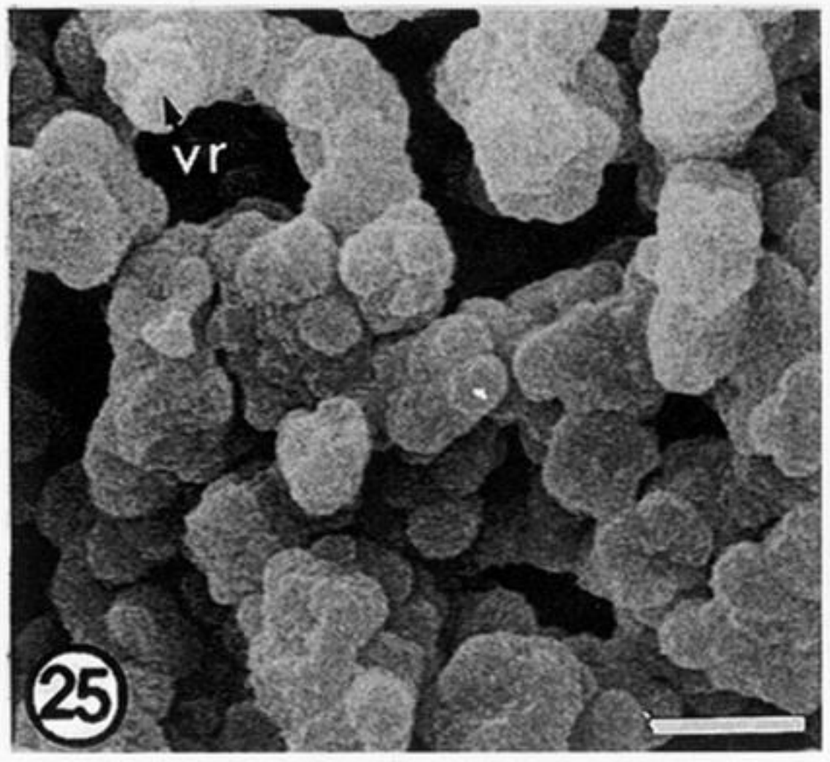

Figures 21–25. SEMs of various gold-coated surfaces of valves of *L. squamiformis* from Kinghorn and Calderwood (figures 22 and 24).

Figures 21 and 23. External view and detail of a virgose lamina with rods distributed as low mounds separated by shallow troughs reflecting the microtopography of the secreting plasmalemmas of the outer epithelium; the ring-like arrangement (rs) of spherules is seen in transverse sections of some rods and scattered isolated spherules (sp). Scale bars = 5 μm and 500 nm respectively.

Figure 22. Vertical fracture section of a compact lamina (cl) developed between two thin laminae of rods some of which are curved (cr). Scale bar = 1 μm.

Figure 24. Oblique view of the base of a virgose lamina succeeding a spherular compact lamina (cl) and including some erect rods (er). Scale bar = 1 μm.

Figure 25. External view of a virgose laminae with coalescing vertical rods (vr) and scattered spherules forming a labyrinth. Scale bar = 2 μm .

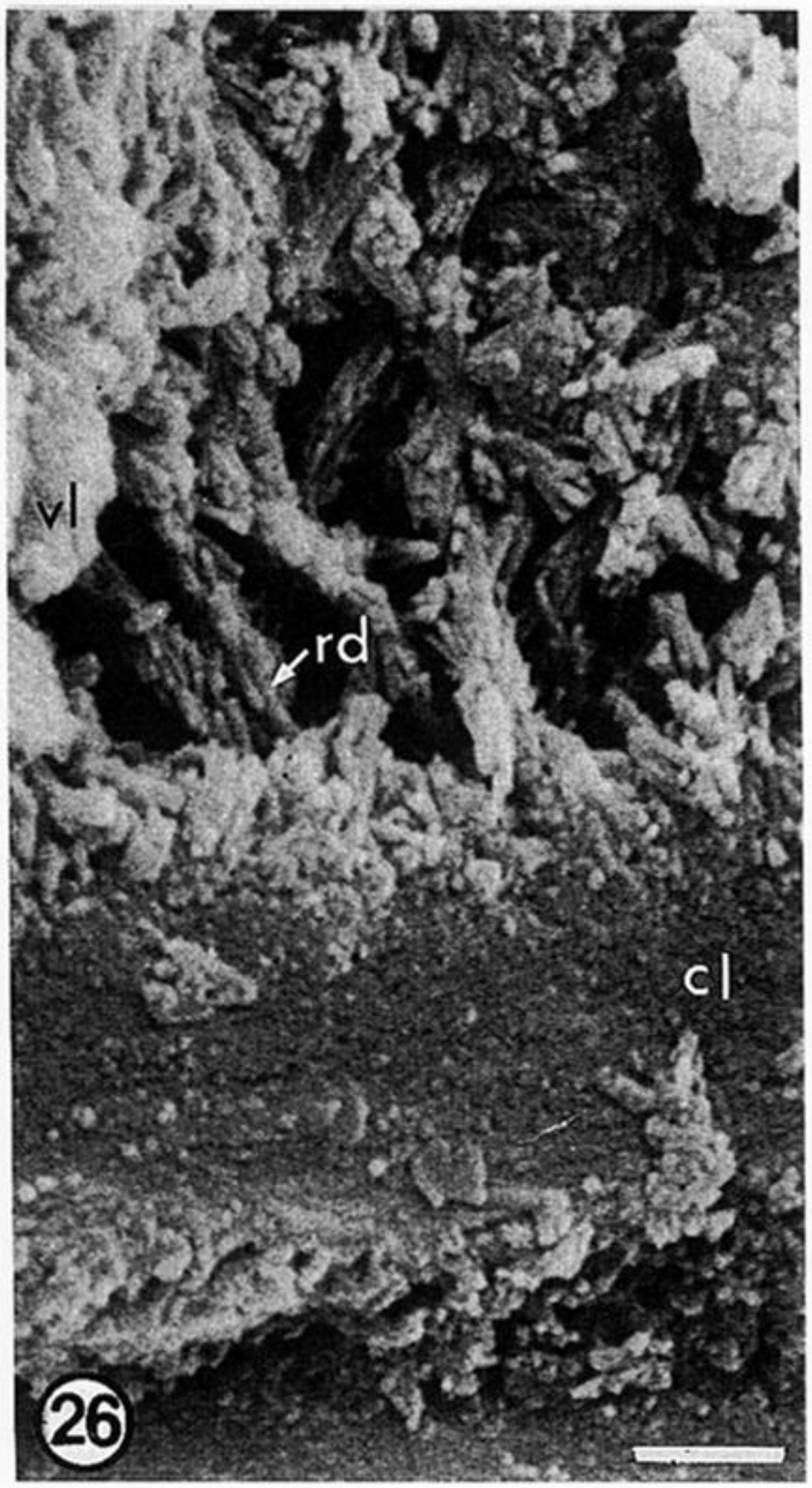

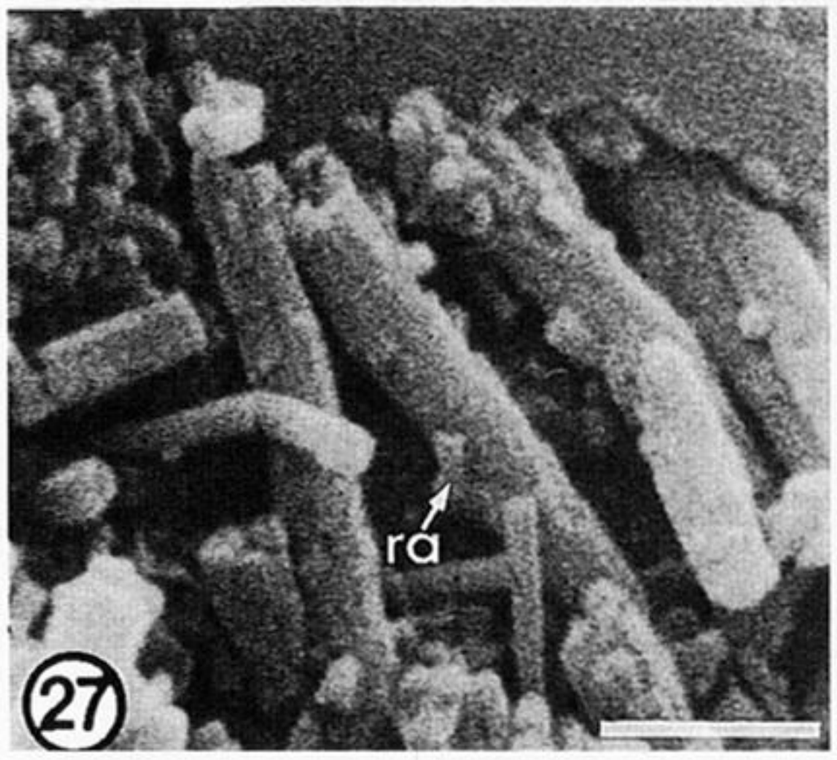

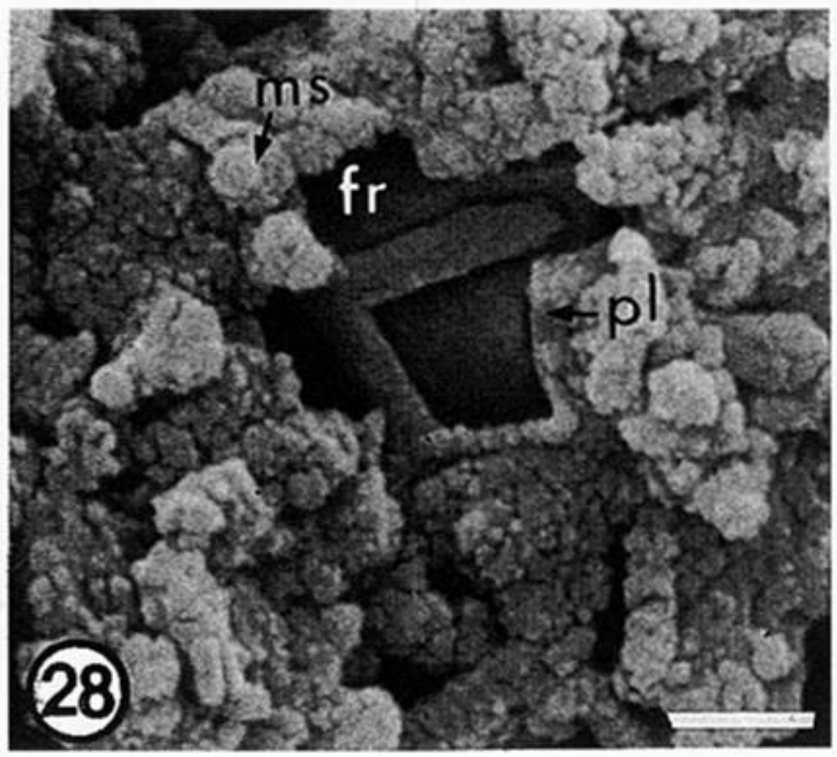

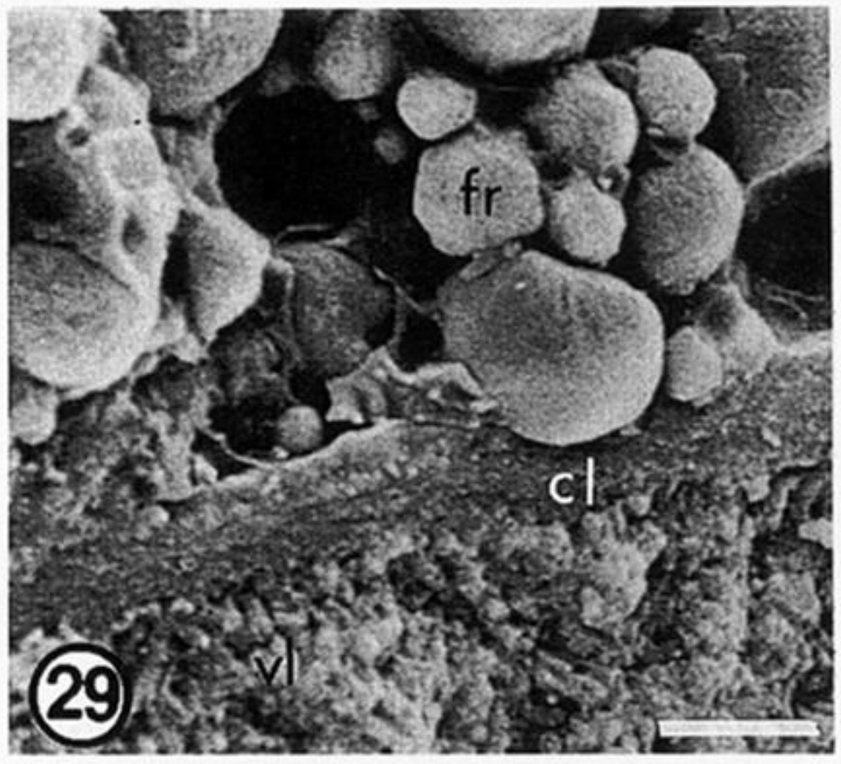

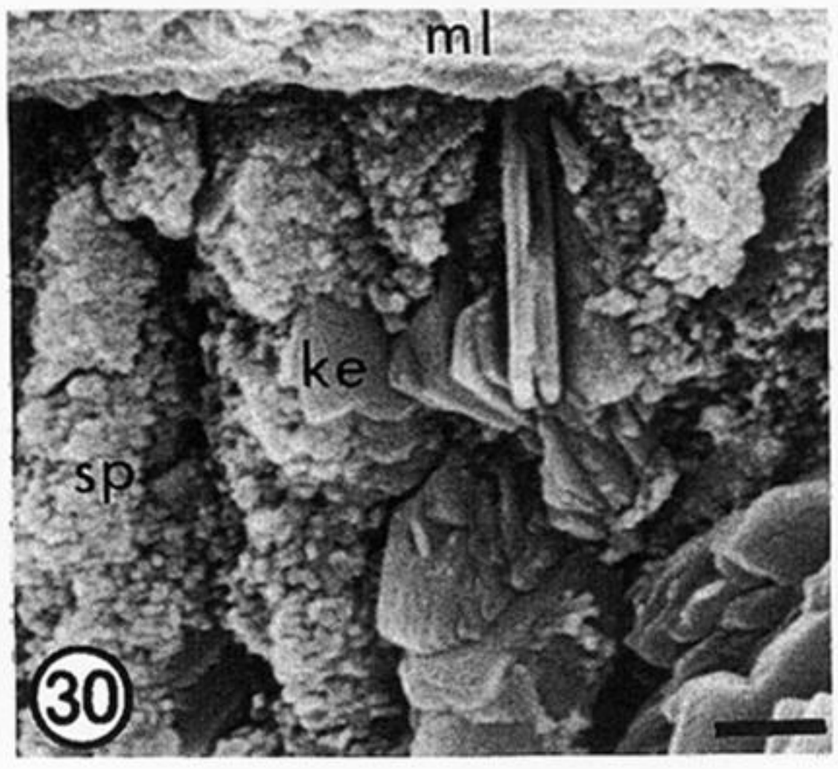

Figures 26–30. SEMs of gold-coated vertical fracture sections of *L. squamiformis* from Calderwood, Kinghorn (figure 28) and Ardross (figure 30).

Figure 26. A virgose lamina (vl) with recrystallized rods (rd) and sparse spherules marking the transition from the underlying compact lamina (cl) composed of spherules and mosaics and containing some recrystallized rods arranged in a lattice. Scale bar = 1 μm.

Figure 27. Recrystallized rods of a virgose lamina, some with superficial second order prisms (ra). Scale bar = 500 nm.

Figure 28. Differentially recrystallized virgose lamina with partly intergrown (pl) clusters of spherular mosaics (ms) and recrystallized prismatic plates engirdling a framboid (fr). Scale bar = 500 nm.

Figure 29. The interface between the matrix of a complete shell, consisting of framboids (fr) cemented by an iron-rich smectite and a recrystallized inner set of compact (cl) and virgose (vl) laminae of the secondary layer of a valve. Scale bar = 5 μm.

Figure 30. Kaolinitic plates (ke) replacing GAGs to form walls alternating with partitions of spherular apatite (sp) within a membranous lamina (ml). Scale bar = 1 μm.

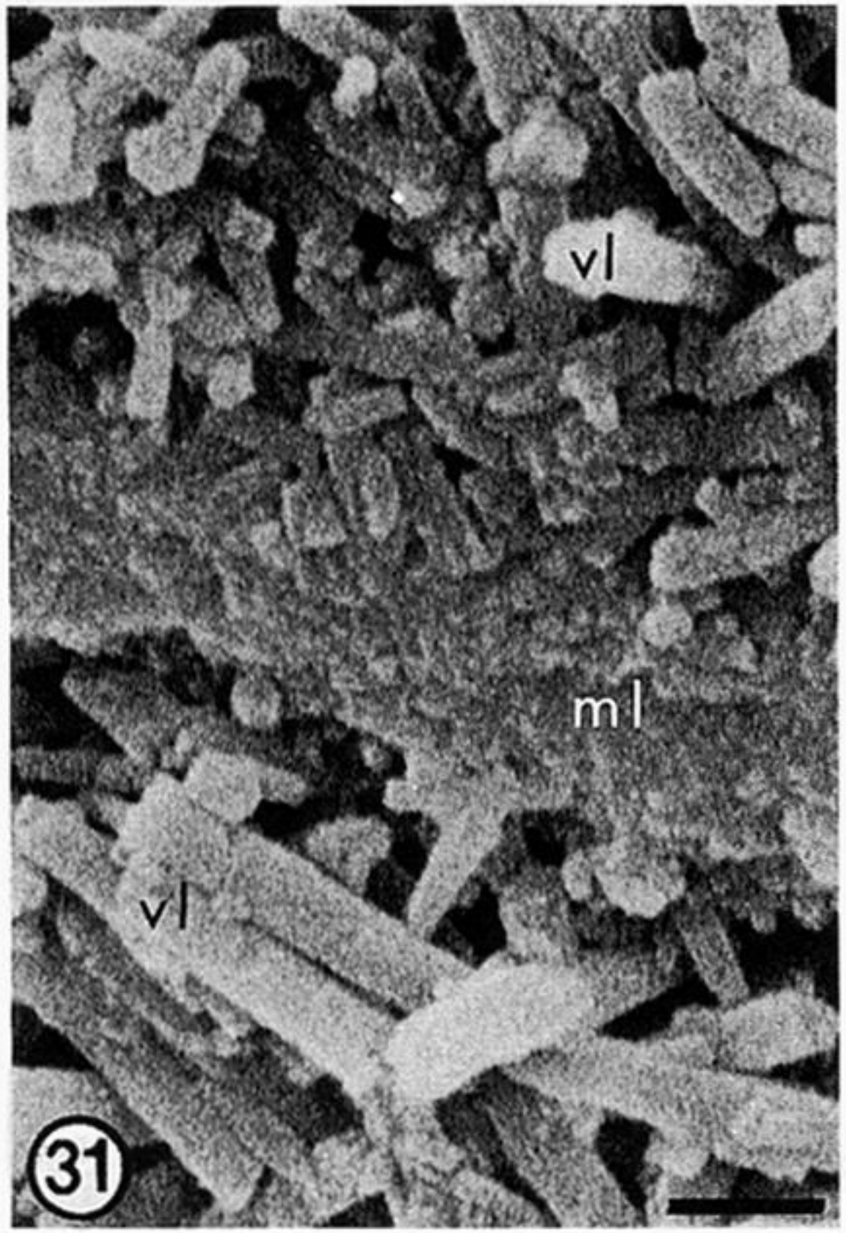

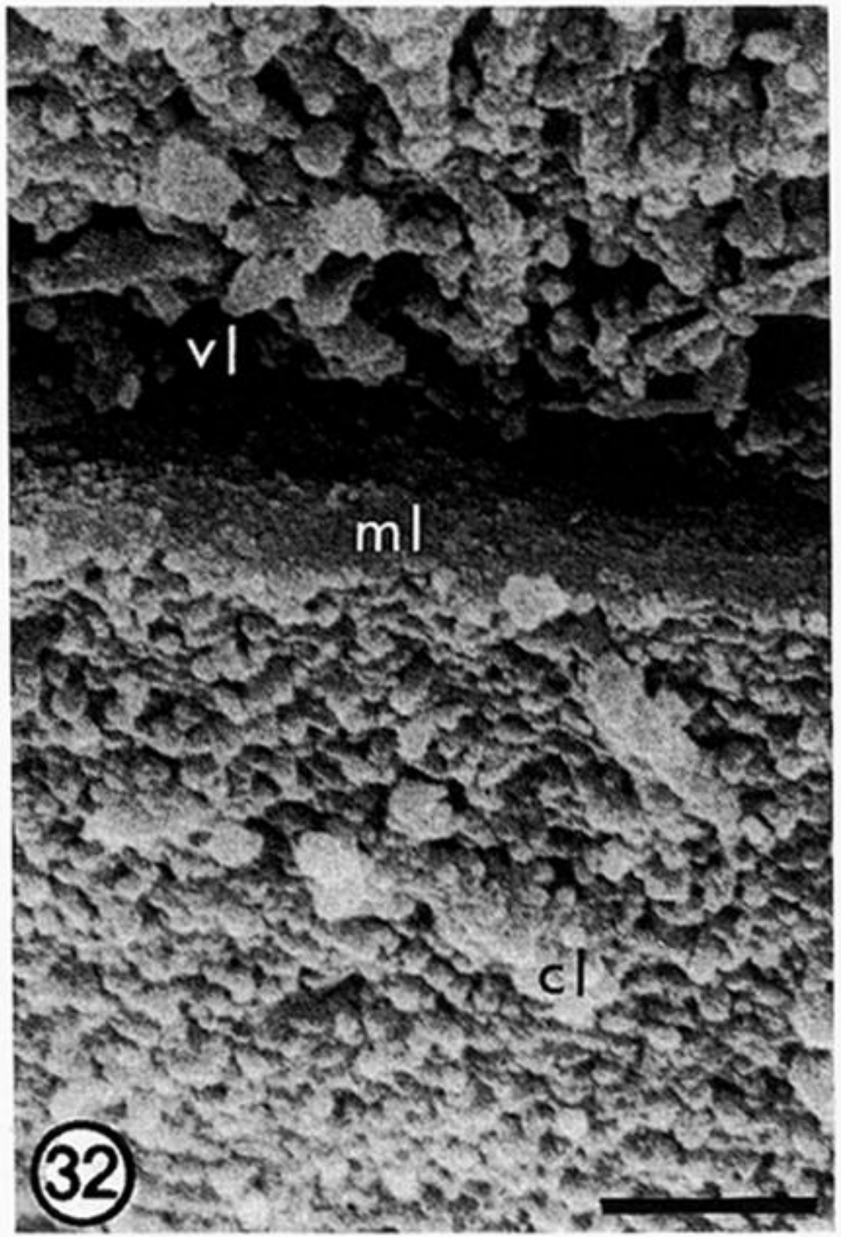

Figures 31–33. SEMs of vertical and oblique fracture sections of membranous laminae in the secondary layers of valves of *L. squamiformis* from Kinghorn and Calderwood (figure 33).

Figure 31. Phosphatized membranous lamina (ml) between two virgose laminae (vl). Scale bar = 500 nm.

Figure 32. Phosphatized membranous lamina (ml) between compact (cl) and virgose (vl) laminae. Scale bar = 1 μm.

Figure 33. Oblique view of the external surface of a compact lamina (cl) with adherent fragments of a lithified membranous lamina (ml). Scale bar = 1 μm.

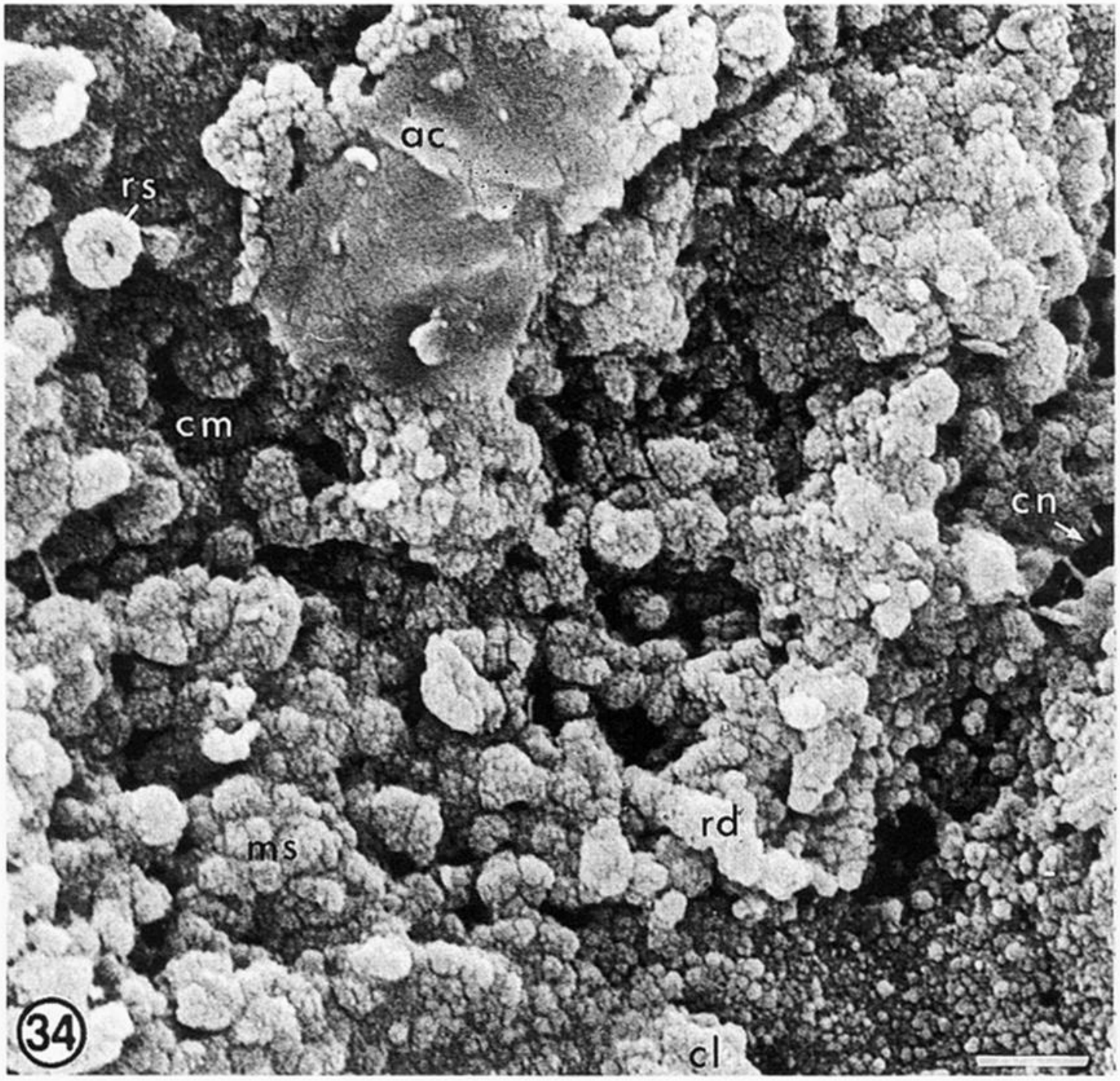

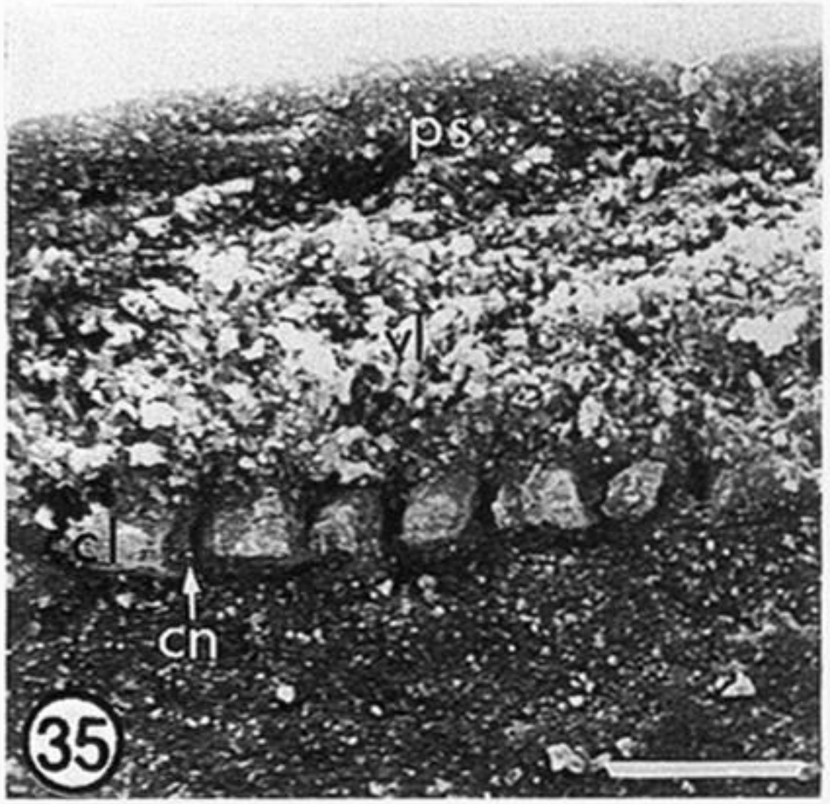

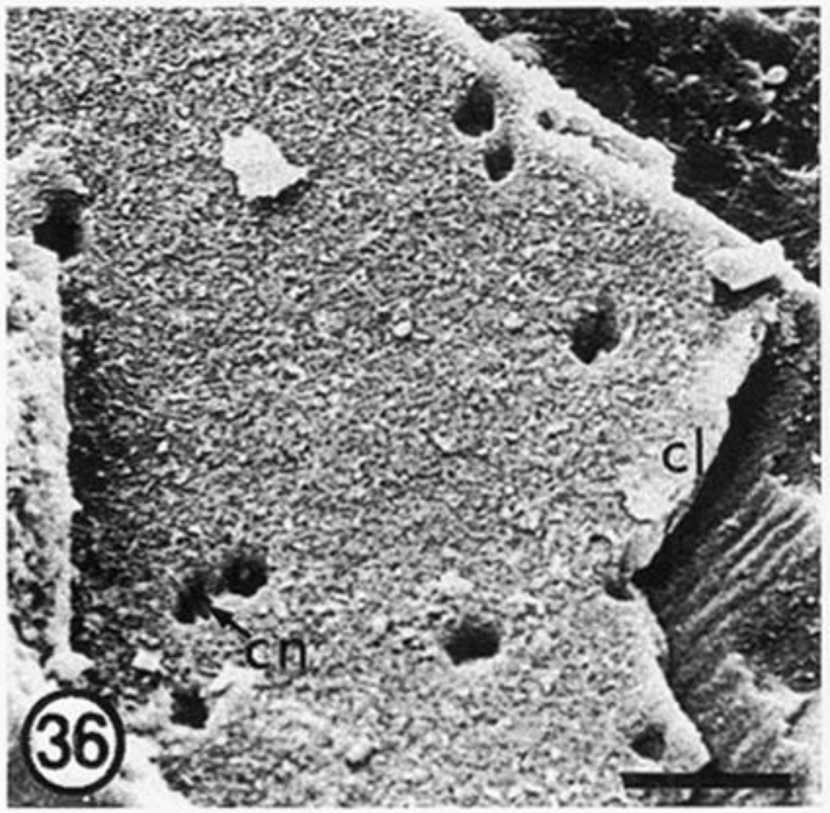

Figures 34–36. SEMs of gold-coated vertical and oblique fracture sections of valves of *L. squamiformis* from Kinghorn (figure 34) and Calderwood.

Figure 34. Details of a virgose lamina succeeding a compact lamina (cl) showing a canal (cn) traversed by an 'organic' strand, rods (rd), mosaics (ms), rings of spherular apatite (rs), a sheet of recrystallized apatite with clay traces (ac) and a chamber (cm). Scale bar = 1 μm.

Figure 35. A compact lamina (cl) perforated by canals (cn) and underlying the standard outer succession of primary layer (ps) and a virgose lamina (vl). Scale bar = 5 μm.

Figure 36. The external surface of a compact lamina (cl) perforated by canals (cn). Scale bar = 10 μm.

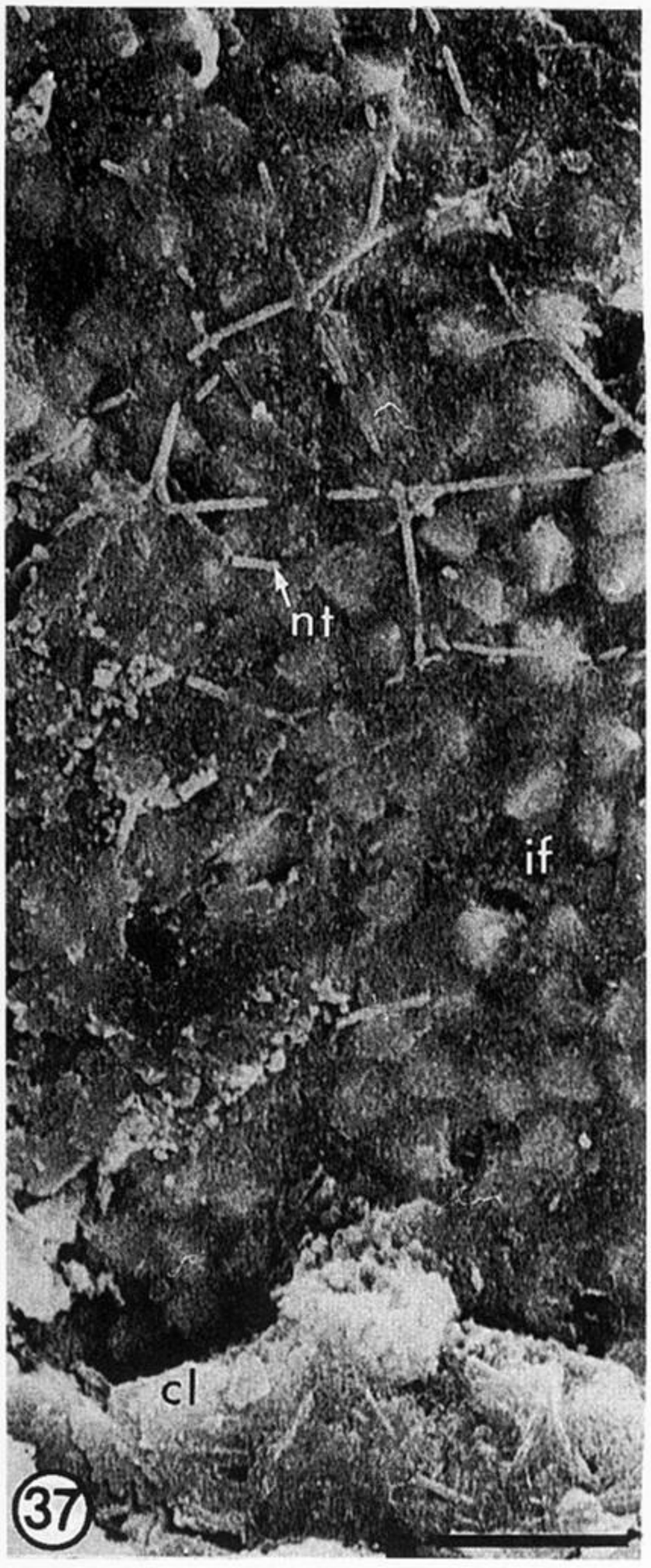

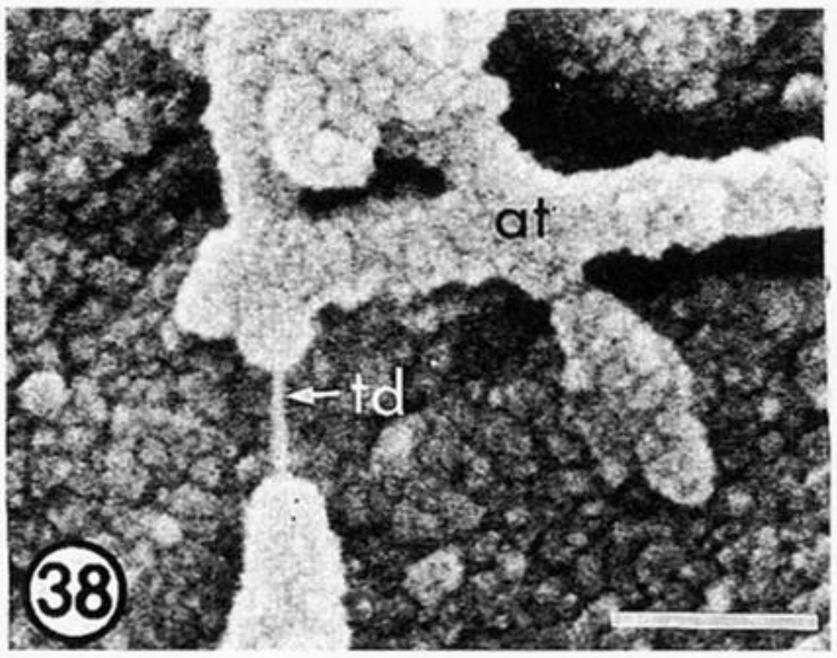

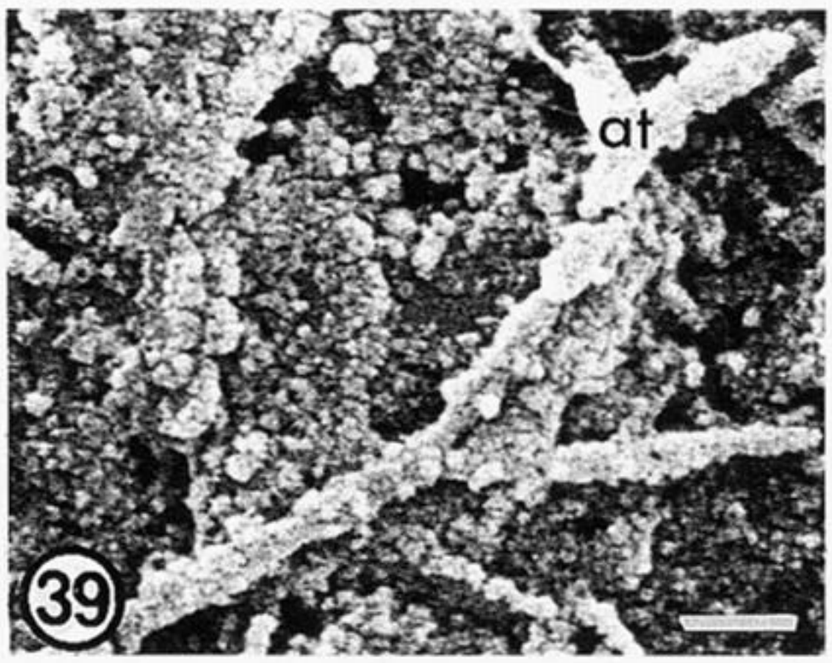

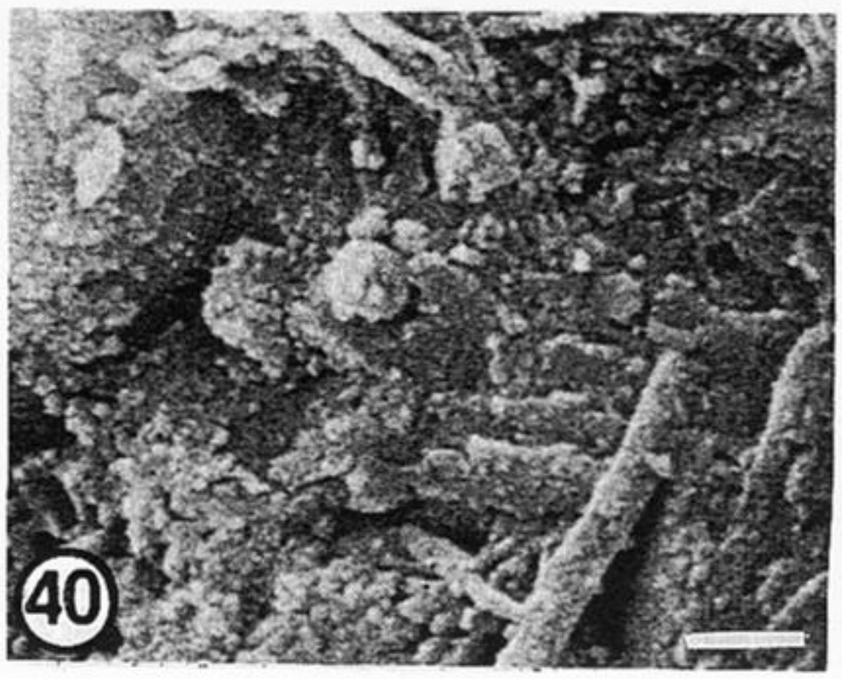

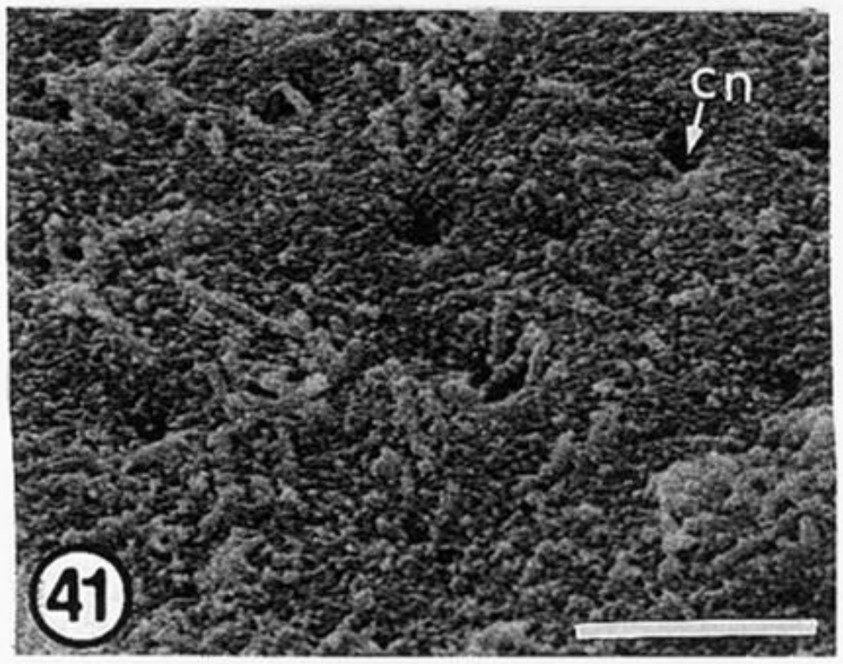

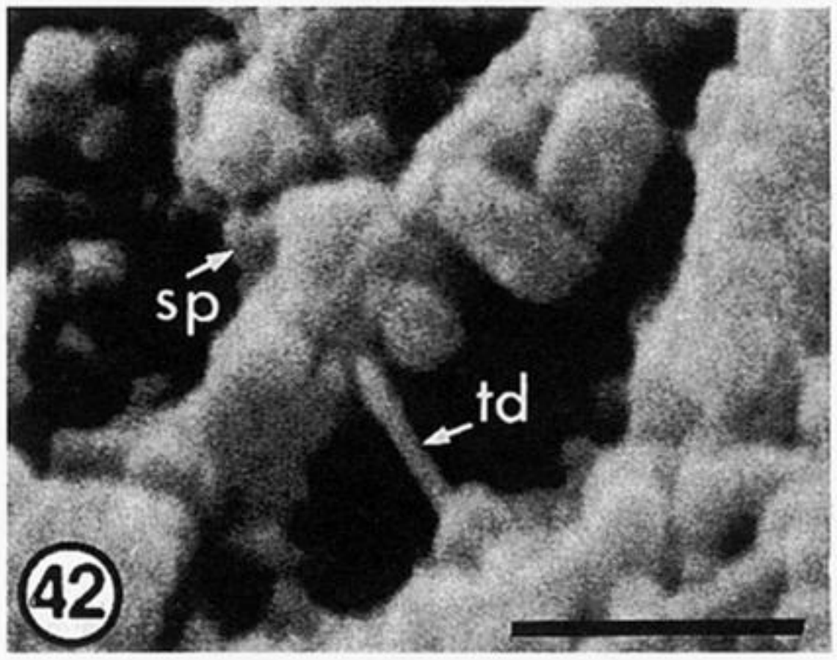

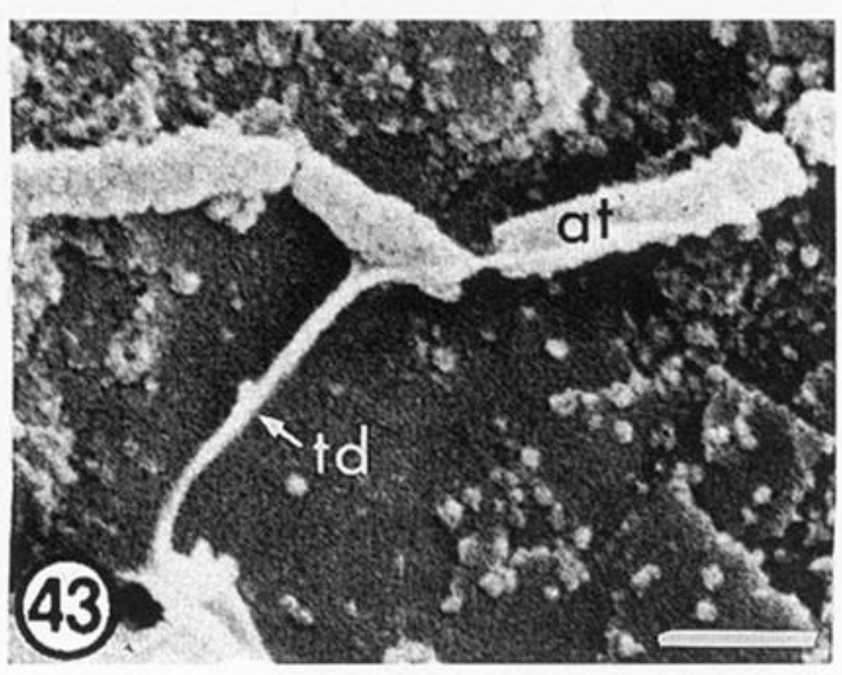

Figures 37–43. SEMs of gold-coated surfaces exposed in an oblique fracture section of the secondary layer of the valve of *L. squamiformis* from Kinghorn.

Figure 37. The external view of the interface between a matrix of illite and framboids (if) with adherent traces of a network of rods (nt) and the innermost compact lamina (cl). Scale bar = 5 μm.

Figures 38, 39 and 43. Details of the network of rods showing the nature of the spherular apatitic coats (at) encasing threads (td) presumably of organic origin. Scale bars = all at 500 nm.

Figure 40. Detail of the external surface of the compact layer seen at the bottom of figure 37, showing rods similar to those forming the network in figure 37. Scale bar = 500 nm.

Figures 41 and 42. General external view and detail of the canaliculate (cn) interface between a compact and virgose laminae showing spherules (sp) forming incipient rods and 'organic' threads (td). Scale bars = 5 μm and 500 nm, respectively.

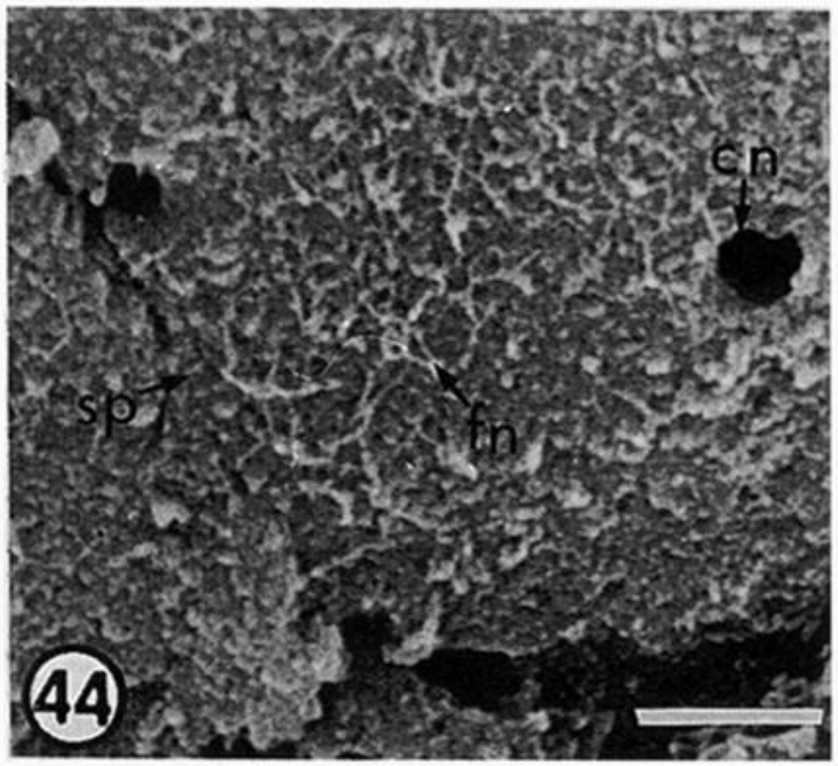

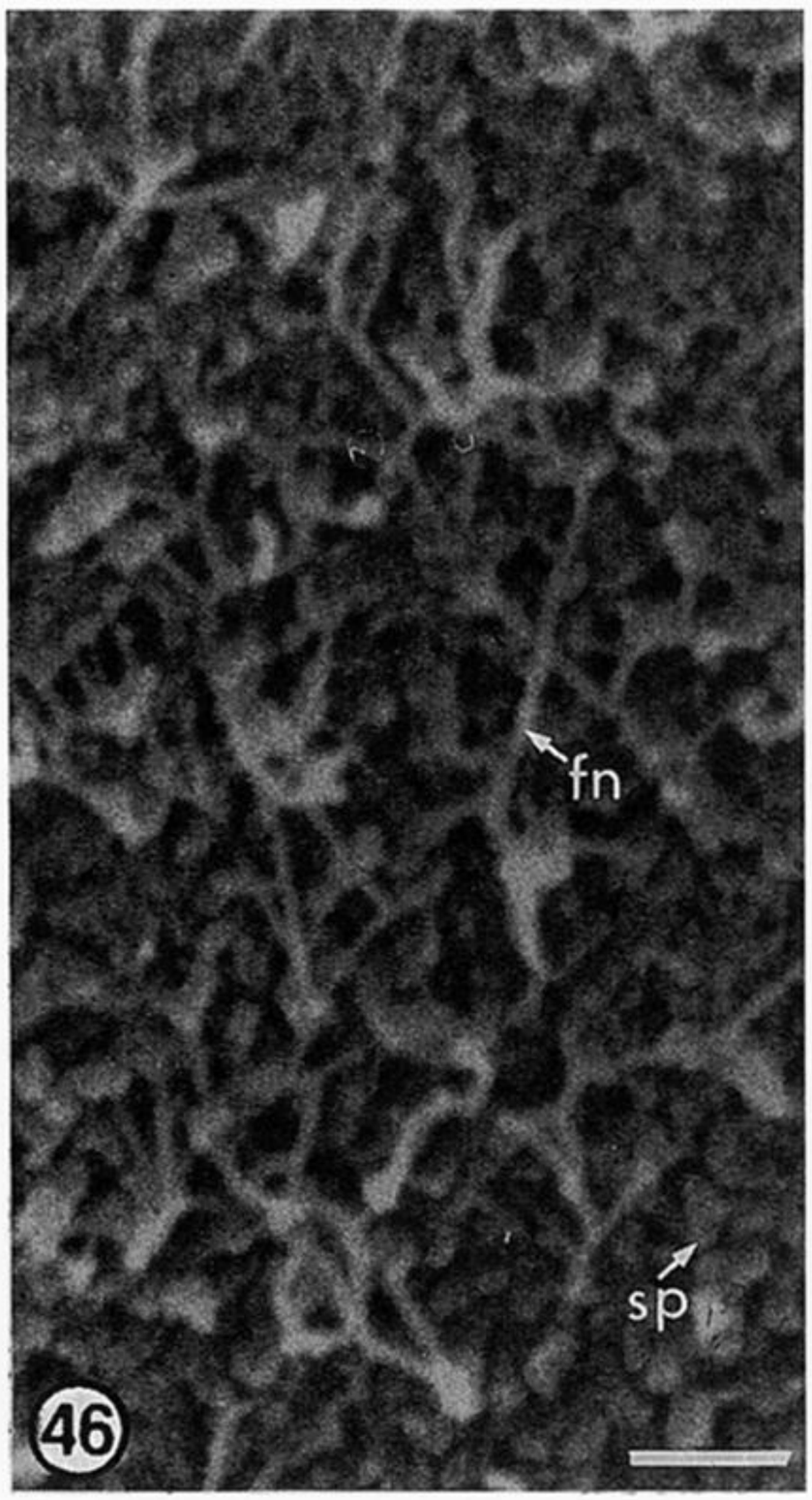

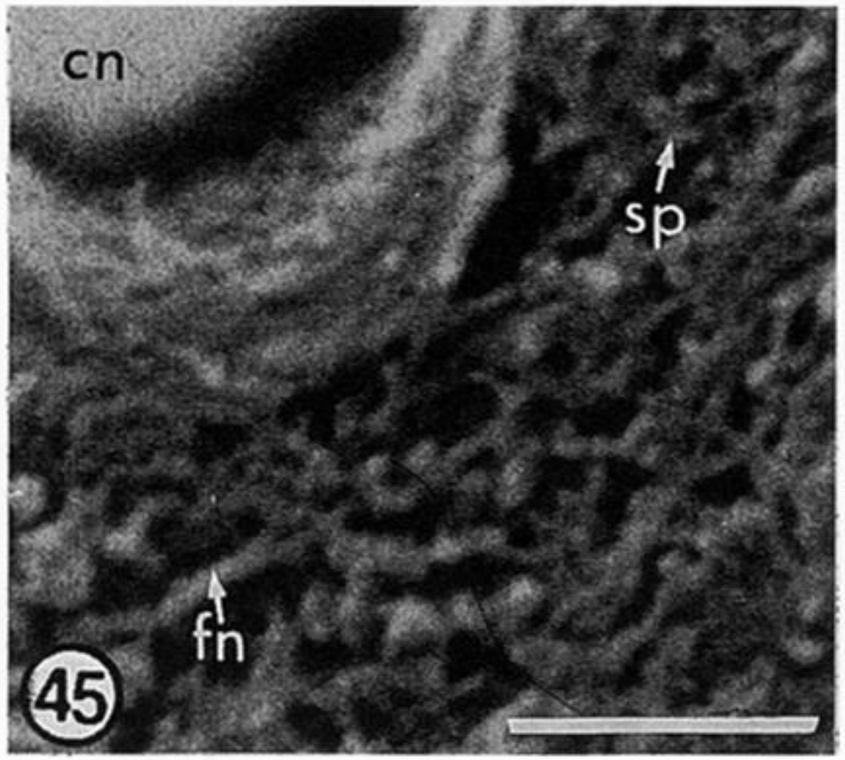

Figures 44–47. SEM of a filamentous network, interpreted as traces of the cell cortex within the shell successions of *Glottidia pyramidata* and *Lingula anatina* (figure 47).

Figures 44–46. Views of the interface between an inner membranous lamina and an outer virgose lamina, in a cut posteriomedian section of a dorsal valve digested in proteinase-k, showing a filamentous network (fn) in relation to canals (cn) and spherular apatite (sp). Scale bars = 1 μm, 500 nm and 250 nm respectively.

Figure 47. A filamentous network (fn) with some GAGs (gg) on a substrate of spherular apatite (sp) exposed below exfoliated periostracum and primary layer in the median part of the external surface of a critical point dried valve previously stored in ethanol (70% by volume). Scale bar = 1 μm.